DETERMINING THE ACCURACY OF SOLAR TRACKERS

A Thesis by
MUHAMMAD SAMI SABRY

Submitted to the Graduate School
Appalachian State University
In partial fulfillment of the requirements for the degree of
MASTER OF SCIENCE

August 2013
Department of Technology and Environmental Design

DETERMINING THE ACCURACY OF SOLAR TRACKERS

A Thesis by
MUHAMMAD SAMI SABRY
August 2013

APPROVED BY:

_____
Brian W. Raichle
Chairperson, Thesis Committee

_____
Marie C. Hoepfl
Member, Thesis Committee

_____
Dennis M. Scanlin
Member, Thesis Committee

_____
Jeffrey S. Tiller
Chairperson, Department of Technology and Environmental Design

_____
Edelma D. Huntley
Dean, Research and Graduate Studies

Abstract

DETERMINING THE ACCURACY OF SOLAR TRACKERS

Muhammad Sami Sabry

B.S., Ain Shams University

M.S., Appalachian State University

Chairperson: Brian W. Raichle

The direct understanding of the expression “accuracy of solar trackers” is that “the trackers follow the sun.” Many studies have used the power produced by the solar trackers as a measure to define and determine a tracker’s accuracy. No studies have been found that determine the accuracy of solar trackers by measuring the tracker angles.

This study was an experiment to measure the tracker angles of the commercially available, non-algorithm based solar trackers located at the Appalachian State University Solar Research Laboratory. The solar trackers were a Zomeworks UTR-200 passive one inclined axis solar tracker and a Wattsun AZ-225 active electro-optical two axis (Azimuth/Altitudes) solar tracker. The measured tracker angle of the passive tracker was the azimuth angle. The measured tracker angles of the active tracker were the azimuth and the altitude angles. The tracker angles of the two trackers were measured under varying conditions, such as different Direct Beam Fractions (DBFs), different total irradiances, different wind speeds, different wind directions, and different times of the day. The angles measured were compared to those calculated by Michalsky’s celestial algorithm, which is “an algorithm for the calculation of solar position that has a stated, and partially

demonstrated, accuracy of 0.01 deg until the year 2050" (Michalsky, 1988, p. 227) in order to determine the accuracy of the solar trackers. Resistance measurements were used to measure the angles of the trackers.

Results were obtained after the verification and the filtration processes of the raw data collected had been carried out. The results showed that the average accuracy of the azimuth angle of the Zomeworks UTR-020 is 75%, the average accuracy of the azimuth angle of the Wattsun AZ-225 is 88%, and the average accuracy of the elevation angle of the Wattsun AZ-225 is 89%. In addition, the results showed a weak correlation between the accuracy of the azimuth angle of the Zomeworks solar tracker and the Direct Beam Fraction (DBF) percentage, a strong correlation between the accuracy of the azimuth angle of the Wattsun solar tracker and the DBF %, and a moderate correlation between the accuracy of the elevation angle of the Wattsun solar tracker and the DBF%. Moreover, the accuracy of the azimuth angle of the Wattsun AZ-225 solar tracker was always higher than that of the Zomeworks UTR-020 under any DBFs and any Global Horizontal Irradiations (GHIs). The results showed also that there was very weak correlation between the accuracy of the azimuth angle of the Zomeworks solar tracker and the ambient temperature, and weak correlations between the accuracies of the angles of the Wattsun AZ-225 and the ambient temperature as well.

Dedication

If she didn’t exist in life, I would create her. Without her being in my life, without her love, and without her owning my heart, I wouldn’t survive anymore. This is Engy, my fiancée, my soul-mate, and my angel who I met when I returned to my country of birth, and who provided me with support and hope. I dedicate to her this thesis, and dedicate for her my life.

Acknowledgements

Because I like their ways of teaching, I would like to be like them and give my academic field a lot, much as they have. These are my professors who were members of my thesis committee.

I would like to thank Professor Brian Raichle for his help and effort in advising, guiding, and supervising my work throughout the time of this study as my direct advisor and the chairperson of my thesis committee. I would like to thank him for being patient when I ask lots of questions to clearly understand very detailed points during this study, or show my opinion in other situations during carrying out the experiments of this study.

I would like to thank Professor Marie Hoepfl for her effort, help, generosity, and permanent caring about my inquiries and concerns as a member in my thesis committee, and as my M.S. program's initial academic advisor. She provided me with a suitable environment to pursue good standing in the program, when I first returned to the USA and began the program until I finished this study and graduated.

I would like to thank Professor Dennis Scanlin, first for his kind acceptance to be a member in my thesis committee as an expert in Renewable Energies, second for his effort and help in advising me as a member in the committee, and finally for his efforts and love to appropriate technologies and renewable energies throughout his exemplary academic history.

I would like to send special thanks to my family who raised me and provided me the opportunity to return to the USA and pursue my graduate studies. I would like to thank my dear friends and my cohort friends in the Department of Technology and Environmental Design for their love, help, and standing beside me. In addition to my friends, I would like to send special thanks, full of gratitude and love, to my fiancée who was with me and in my heart while working on this study, and studying in the M.S. program.

Finally, I would like to thank the Appalachian State University Energy Center for funding the Appalachian State University Solar Research Facility in part with the Department of Technology and Environmental Design.

Table of Contents

List of Tables

List of Figures

CHAPTER 1: INTRODUCTION

Interest in solar energy has grown for a variety of reasons. It is a sustainable energy resource, it produces no air pollution, and it is increasingly affordable and reliable. Use of solar energy can help to mitigate greenhouse gases, and therefore many policies have been developed and adopted, and many projects have been undertaken worldwide to produce solar energy and to reduce the production of greenhouse gases.

Photovoltaic (PV) technology has continued to develop in recent years. Tracking technology that maximizes the power output of PV panels is just one area of improvement. PV manufacturers claim the increase in power generated from a PV panel mounted on a one-axis solar tracker can be 30% higher than from a fixed (non-tracking) PV panel. In addition, "tests have shown that up to 40% extra power can be produced per annum using a variable elevation solar tracker" (Clifford & Eastwood, 2004, p. 269). Moreover, it is claimed that a mounted PV panel on a two-axis solar tracker will generate 40% more power than a tilted-south fixed panel (Mousazadeh et al., 2009, p. 1814).

To maximize radiation hitting the surface of a fixed PV array throughout the year, the array needs to be adjusted to a certain inclination angle and a certain solar azimuth angle. The inclination or the tilt angle is "the angle between the surface normal and the vertical" (Braun & Mitchell, 1983, p. 439); it is more commonly described as the angle between the horizontal and the tilted plane of the PV array. Solar PV arrays used year-round are normally adjusted to an inclination angle equal to the latitude where the panel is being installed. The solar azimuth angle is "the horizontal angle measured from south (in the northern hemisphere) to the

horizontal projection of the sun's rays" (Mousazadeh et al., 2009, p. 1801) or "the angular distance between true south and the point on the horizon directly below the sun" (Mazria, 1979, p. 656). For northern latitudes due south is typically the best azimuth orientation. Even better performance can be obtained if an array tracks the sun throughout the day and continually adjusts its azimuth and/or inclination angles. By adjusting these angles, the sun incidence angle becomes closer to 0^{O} and the direct solar radiation is more normal or perpendicular to the array's surface throughout the day and thus better energy output will result. The sun incidence angle is the angle "measured between a ray from the sun and the surface normal" (Braun & Mitchell, 1983, p. 439). The surface normal is the imaginary line perpendicular to the PV array's surface. For a fixed orientation array that is not adjusted, the sun incidence angle changes throughout the day. This leads to less energy generation because of the decrease of the array's effective area normal to the solar radiation.

One low-tech method to increase an array's effective area is with periodic manual inclination angle adjustments. In summer, manufacturers recommend the inclination angle be decreased because of the high elevation of the sun above the horizon. In winter, manufacturers recommend the opposite because of the low elevation of the sun above the horizon. To set the azimuth angle, manufacturers recommend the surface on which the PV panel is fixed to be directed towards the south (in the northern hemisphere) or towards the north (in the southern hemisphere).

The tracking accuracy refers to the capability of trackers to point to the sun no matter what the trackers' control scheme is. To achieve high accuracy, the PV array mounted on the tracking system must be close to normal to the direct radiation throughout the day. Knowing the tracking accuracy will be helpful to potential adopters of PV tracking systems.

Solar tracking PV systems continually follow the position of the sun in the sky. A variety of tracking control schemes exist, including algorithm-based, thermal, and electro-optical systems. An algorithm-based control scheme on a solar tracker provides the equations through which the inclination and azimuth angles are calculated and employs active positioning using electric motors. This guarantees the optimum orientation of the trackers. Non-algorithm based control schemes of solar trackers, such as thermal and electro-optical control schemes, don't involve the use of equations for calculating the inclination and azimuth angles. Instead, they provide active and passive mechanisms by which the trackers follow the sun through the sky. Most residential-scale solar trackers are non-algorithm based control scheme solar trackers. It's important to understand the performance of these trackers and to determine their accuracy.

Statement of the Problem

A tracker's accuracy affects the irradiance intercepted and the energy generated by a PV array. Understanding the accuracy of non-algorithm based solar trackers is necessary for potential adopters to make informed decisions when choosing between various available tracking options. Determining this accuracy can be accomplished through an outdoor experiment that compares the performance of the solar trackers under real life conditions. The amount of the incident total and normal direct beam likely affects the driving mechanisms of the non-algorithm based solar trackers. Hence the total radiation and the Direct Beam Fraction (DBF), or the ratio of the solar direct normal radiation to the total solar radiation, are likely important factors to consider when trying to determine and compare the performance of different PV tracking technologies.

A typical PV tracking system's main components are the tracking device and the tracking algorithm, the control system, the positioning system, the driving system, and the

sensing system (Rockwell Automation, 2009). This type of PV tracking system is typically included in commercial-scale solar plants. However, residential-scale solar trackers are typically not algorithm based for simplicity to the customer and for reduction in the cost of the system. Hence they may not be as accurate as algorithm-based solar trackers. The problem this study addresses is to determine the accuracy of such residential trackers, so that the home owners and installers can make better decisions about what residential PV technology to install. No studies determining the tracking accuracy using direct angular observations have been found.

Purpose of the Study

This research compared the accuracy of two solar trackers under the same varying conditions. This research was carried out on a Zomeworks UTR-020 passive azimuth tracker fixed at a 42° altitude angle, and a Wattsun AZ-225 active altitude and azimuth tracker to determine their accuracy with varying DBF, total irradiance, and wind direction at different ambient temperatures.

Research Question and Hypotheses

This research was guided by one primary research question. Three related research hypotheses (H) were generated.

RQ1: What is the accuracy of non-algorithm based one-axis solar trackers and two-axis solar trackers under varying DBF and total irradiance?

$H_{1.}$ There will be strong positive correlations between tracker accuracy and level of DBF for the Wattsun AZ-225 active altitude and azimuth and the Zomeworks UTR-020 passive azimuth solar trackers.

H_2. The Wattsun AZ-225 active altitude and azimuth tracker will be more accurate than the Zomeworks UTR-020 passive azimuth tracker under strong DBFs and total irradiances.

H_3. There will be weak correlation between the accuracy and the ambient temperature.

Definition of Terms

Direct Beam Radiation: "The radiation that comes directly from the sun with no scattering in the atmosphere" (Robinson & Raichle, 2011, p.1-2).

Direct Beam Fraction (DBF): The ratio of the vertical component of the Direct Normal Irradiation DNI to the Global Horizontal Irradiance GHI.

Direct Normal Irradiation (DNI): "The flux of the beam radiation through a plane perpendicular to the direction of the sun" (Reno, Hansen, & Stein, 2012, p. 9).

Elevation Angle (Altitude Angle) α: "The vertical angle between the projection of [the] sun's rays on the horizontal plane and direction of [the] sun's rays passing through the point" (Braun & Mitchell, 1983, p. 439).

Global Horizontal Irradiance (GHI): "The sum of the diffuse radiation incident on a horizontal surface plus the…[vertical component of the direct normal irradiance]…" (Reno et al., 2012, p. 9).

Inclination Angle (Slope of the Surface) β: "The angle between the surface normal and the vertical" (Braun & Mitchell, 1983, p. 439).

Sun Incidence Angle θ: "The incidence angle, θ, is measured between a ray from the sun and the…[normal of the PV array]…" (Braun & Mitchell, 1983, p. 439).

Sky Diffuse Radiation: "The solar radiation received…[by a surface]…from the sun after its direction has been changed by scattering by the atmosphere" (Helwa, Bahgat, El Shafee, & El Shenawy, 2000, p. 37).

Solar Azimuth Angle γ_s: "The horizontal angle measured from south (in the northern hemisphere) to the horizontal projection of the sun's rays" (Mousazadeh et al., 2009, p. 1801).

Surface Azimuth Angle γ: "The angle between local meridian and the horizontal projection of the surface normal" (Braun & Mitchell, 1983, p. 439).

Surface Elevation Angle $\alpha_{surface}$: The vertical angle between the surface and the horizontal plane.

Readers can refer to Figures 1, 2, & 3 for a graphical representation of the above defined angles, an understanding of which was critical to carrying out this study.

Limitations of the Study

The first limitation of the study was that it was done only on a Wattsun AZ-225 active altitude and azimuth tracker and a Zomeworks UTR-020 passive azimuth tracker at one location: Boone, North Carolina. Therefore, the findings from this study apply only to these trackers, at Boone's latitude of 36.2167^{O}N. Another limitation was the potential angle offset produced by the Zomeworks UTR-020 passive azimuth tracker to follow the motion of the sun because of the weight of the 6" linear potentiometer mounted on it, and the friction that took place due to the relative motion between the inner and outer damper rods (Refer to Chapter 3, Calibration of the 6" Linear Potentiometer). A third limitation was that the study was carried out in an outdoor environment, which meant that light, wind, and other weather-related variables could not be controlled; however, one of the goals of this research was to examine the accuracy in a real-world situation, so the findings of this research lend greater insight into the tracking accuracy of these systems in regular use.

Significance of the Study

This study filled a gap in the literature and directly described and determined the accuracy of solar trackers by measuring their tracking angles. No previous studies were found that had tried that approach, although many studies have documented the benefits of using tracking devices to increase the power output of solar panels. Through this study, residential PV system owners may be able to make better-informed decisions about whether it is better to install a fixed, one-axis tracker, a two-axis tracker, or even no PV system in a certain site based on a more complete study of the performance of these systems and their corresponding economic values. Because tracker performance will be characterized according to climatic conditions, extrapolation to other locations with known climatic conditions should be possible.

CHAPTER 2: REVIEW OF LITERATURE

Solar Irradiation and Meteorological Conditions

As solar radiation passes through the atmosphere it is scattered due to collisions with air molecules in the atmosphere and thus the incidence angle changes, making the solar rays diffuse rather than direct (Robinson & Raichle, 2011). If the weather is windy, cloudy, rainy, or snowy, there will be more scattering, reflections, and inter-reflections of solar rays. Hence, the terms Direct Radiation, Diffuse Radiation, Albedo, and Direct Beam Fraction (DBF) came into focus for scientists and researchers interested in the solar energy discipline. Direct radiation is "the radiation that is not reflected or scattered and reaches the surface directly" (Mousazadeh et al., 2009, p. 1801). Diffuse radiation is "radiation that has been scattered either by clouds, rain, or any other potential hazard" (Robinson & Raichle, 2011, p. 1). The albedo is defined as "the fraction of radiation reaching the ground that is reflected back to the atmosphere from which a part is absorbed by the receiver" (Mousazadeh et al., 2009, p. 1801). The amount of direct or diffuse radiation depends on the position of the sun, atmospheric conditions, and the orientation of the surface of the PV array. The ground reflected radiation depends on the environmental factors between the surface of the PV array and the ground (Braun & Mitchell, 1983, p. 440 & 441).

Solar Tracking Geometry

For the surface of a PV array, it is important to know its azimuth and inclination angles, as shown in Figure 1. For the position of the sun, it is important to know the solar azimuth and solar elevation angles, as shown in Figure 2. Understanding the relationship between these sun angles and the orientation of the solar panels is fundamental to determining tracker accuracy. In order to have an optimum tracking orientation of the solar tracker and insure that the surface of the PV array is always normal to the incident solar radiation as shown in Figure 3, the inclination angle and the solar elevation angle should be complementary angles (their sum is equal to 90°) and the surface azimuth angle should be equal to the sun azimuth angle (Braun & Mitchell, 1983, p. 444).

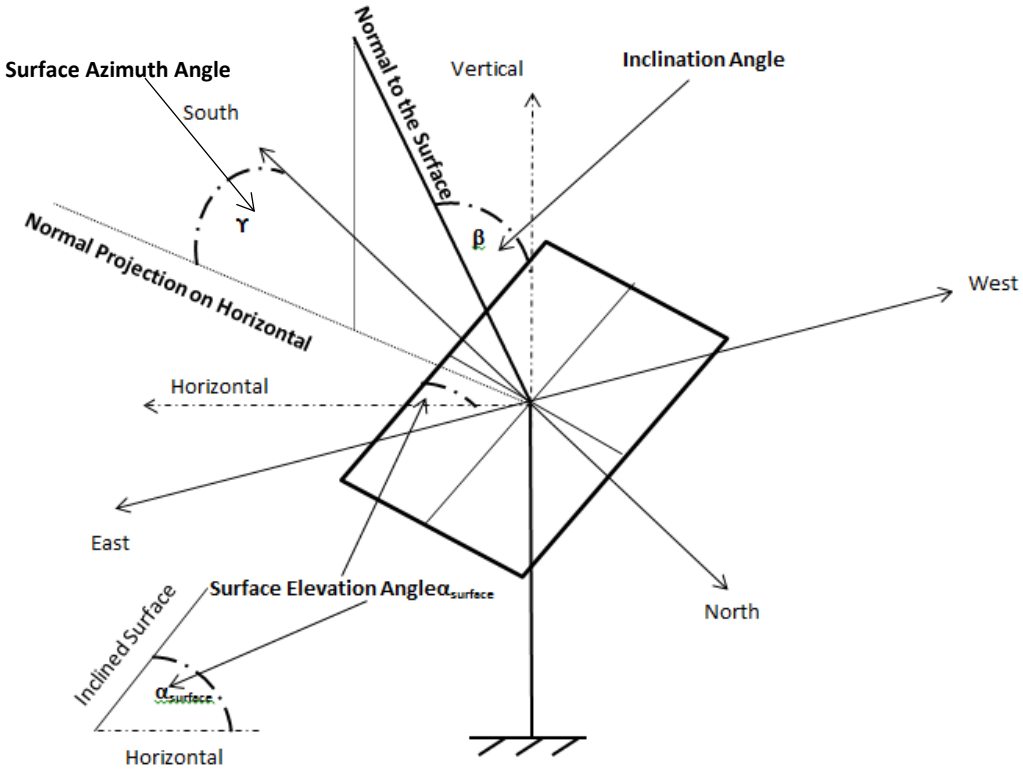

Figure 1. Surface azimuth and surface elevation angles.

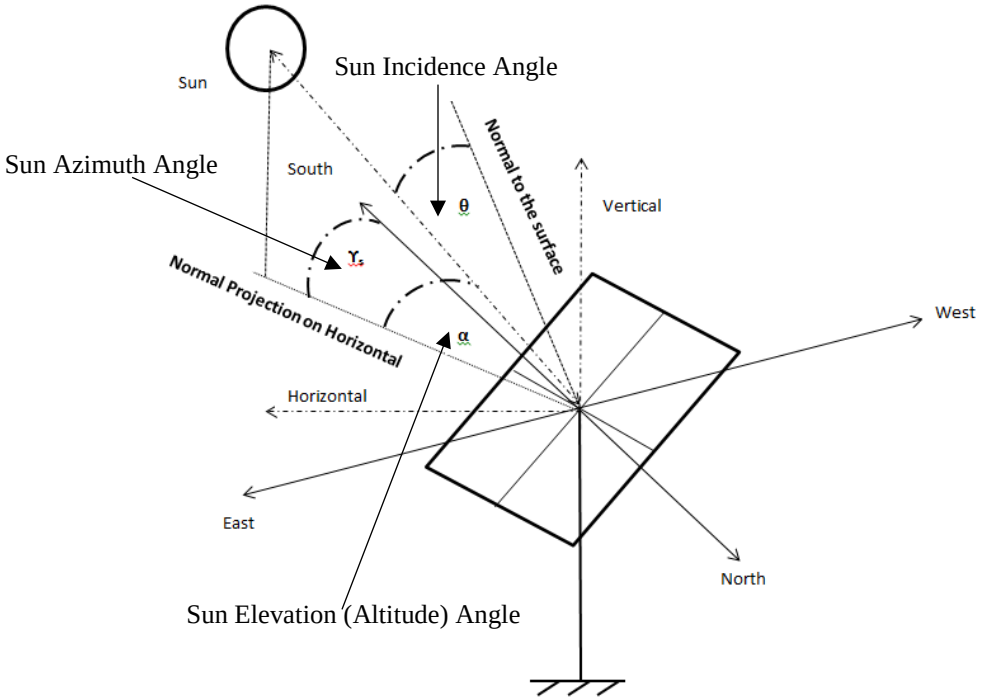

Figure 2. Solar azimuth, solar elevation, and solar incident angles while the direct solar radiation is not normal to a surface (general condition).

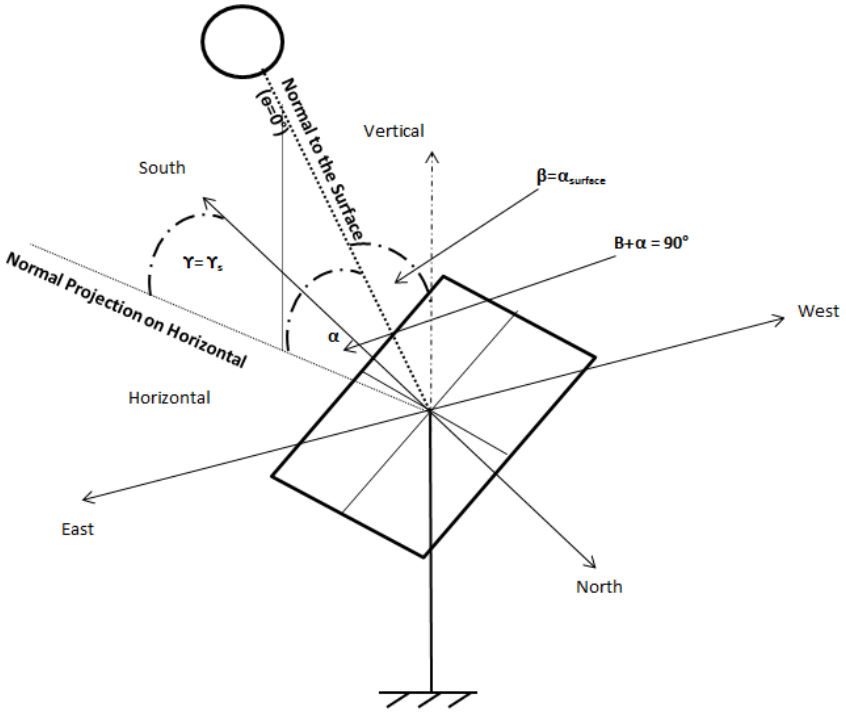

Figure 3. Optimum tracking orientation; that is, direct radiation normal to the surface.

Components of the Solar Tracking System

The main components of a typical commercial solar tracking system are the tracking device, the tracking algorithm, the control unit, the positioning system, the driving mechanism, and the sensing devices. The main components of a typical residential solar tracking system are the tracking device, the non-algorithm based control scheme (whether thermal or electro-optical), the positioning system, the driving mechanism, and/or the sensing devices. The algorithm is a tracking control scheme that calculates the angles that are used to determine the position of the solar tracker. There are two types of algorithms: astronomical algorithms and real-time light intensity algorithms. The astronomical algorithm is a purely mathematical algorithm based on astronomical references to calculate the solar angles. The non-algorithm thermal control scheme uses differential thermal expansion of a working fluid to exert torque to move the tracker. The non-algorithm electro-optical control scheme uses differential optical signal to exert torque on the tracking device to follow the sun.

In an algorithm-based system, the control unit executes the tracking algorithm and manages the positioning system and the driving mechanism so that the tracking device is directed towards the direction calculated. The positioning system is the system that moves the tracking device to face the sun at the calculated angles. The positioning system can be electrical or hydraulic. The driving mechanism is the mechanism that is directly responsible for moving the tracking device to the position determined by the positioning system. The sensing devices comprise a group of sensors that measure the ambient conditions (such as ambient temperature, relative humidity, amount of rain, and other ambient measurements), the light intensity (in the case of real-time light intensity algorithms), and the tilt angle of the tracker. The latter is accomplished by means of an inclinometer or a combination of limit switches and motor encoder counts (Rockwell Automation, 2009).

Solar Tracking Technologies

Solar panels can operate without the use of solar tracking devices, but it is well documented that performance of the system is reduced without the use of trackers (Mousazadeh et al., 2009). This is due to the fact that the earth rotates on its axis and revolves around the sun, so the sun's position in the sky relative to the horizon changes over the course of the year. Therefore, a fixed collector will not be able to maintain a high array effective area with the sun's motion as trackers do (Catarius & Christiner, 2010). Solar tracking technologies are usually classified into passive (mechanical) or active (electrical) devices. They can be further classified into one axis solar trackers or dual axis solar trackers, as shown in Figure 4.

Passive solar trackers are trackers with a rotating motion created by thermal expansion. They contain two identical cylindrical tubes filled with a pressurized fluid (usually Freon) or a shape memory alloy that work as an actuator for the rotation of the passive solar trackers. The pressurized fluid thermally boils and expands in the cylinder exposed to the sun and moves into the other that is shaded from the sun and condenses. This causes unbalanced forces that exert a thermal torque on the tracker towards a certain direction until equilibrium is restored and the actuators are balanced.

Active trackers use a motorized (electrical) motion. "Major active trackers can be categorized as microprocessor and electro-optical sensor based, PC controlled data and time based, auxiliary bifacial solar cell based, and a combination of these three systems" (Mousazadeh et al., 2009, p. 1806). Electro-optical sensor based active trackers contain at the least one pair of connected photo-resistors or PV solar panels. This pair is electrically balanced by equal illumination intensities and so there is no control signal on the driving motor. "These sensors are positioned near one another and have a divider, a tilted mount at a

calculated angle, or use a collimator to create a useful current and/or voltage difference between the two sensors" (Catarius & Christiner, 2010, pp. 7-8). The different setups are shown in Figure 5. For the auxiliary bifacial solar cell active tracker, the bifacial solar cell creates an imbalance in power output and drives the trackers towards the desired position. Poulek and Libra (n.d.) describe an auxiliary bifacial solar tracker. This type of solar tracking basically involves having the tracking/backtracking solar panels connected to a DC motor. "Two antiparallel sensing/driving solar cells are connected to reversible DC motor, [and] the transmission is self-locking" (Poulek & Libra, n.d., p. 4). The figure used by Poulek and Libra to show the principles of the auxiliary bifacial solar tracker is shown in Figure 6. Auxiliary bifacial solar trackers may seem similar to passive solar trackers; however, an auxiliary bifacial solar tracker is moved by an electrically controlled motor, while the passive tracker is moved by a thermally-induced unbalanced torque. As a result the auxiliary bifacial solar trackers are more accurate than passive solar trackers, with an accuracy of about $\pm 5^{O}$ (Poulek & Libra, n.d.). The PC controlled date- and time-based active tracker calculates the angles in terms of date and time by means of algorithms and sends signals to the control unit to manage the positioning system and the driving mechanism so that the tracker is directed to the desired direction (Mousazadeh et al., 2009).

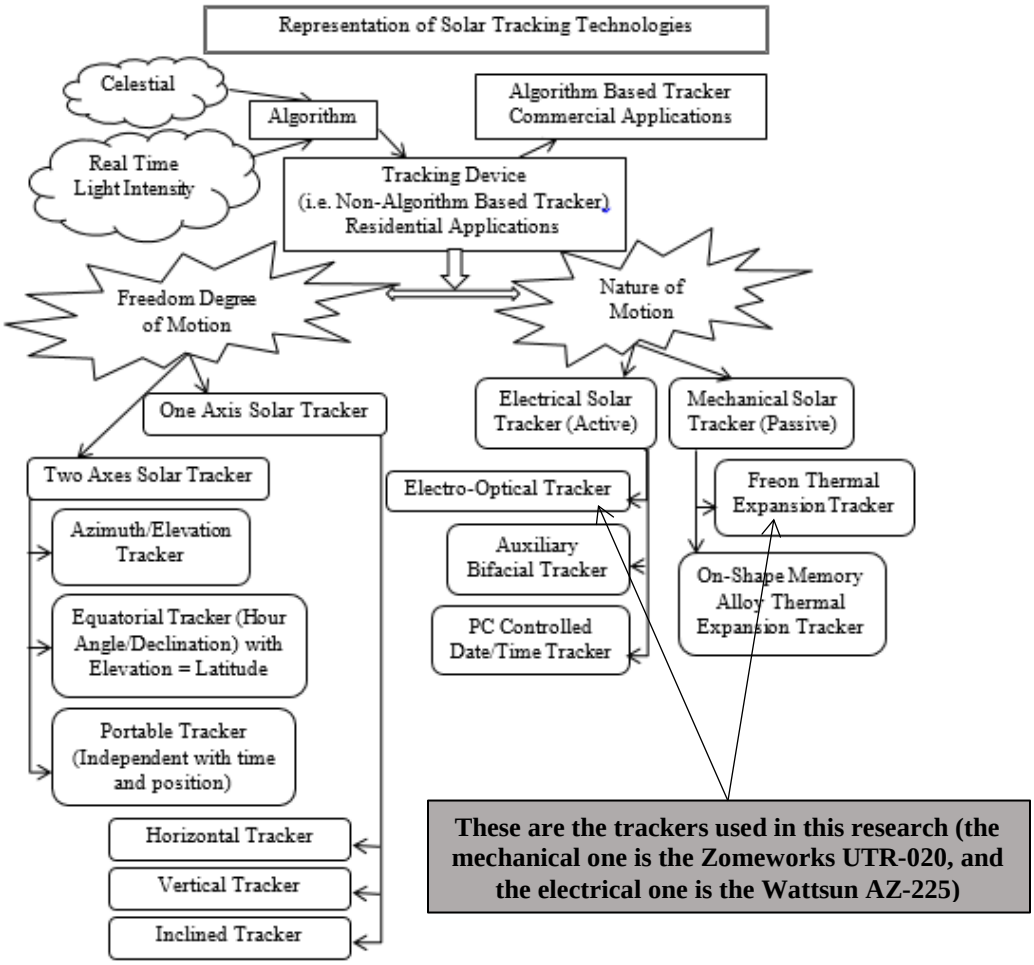

Figure 4. Representation of solar tracking technologies.

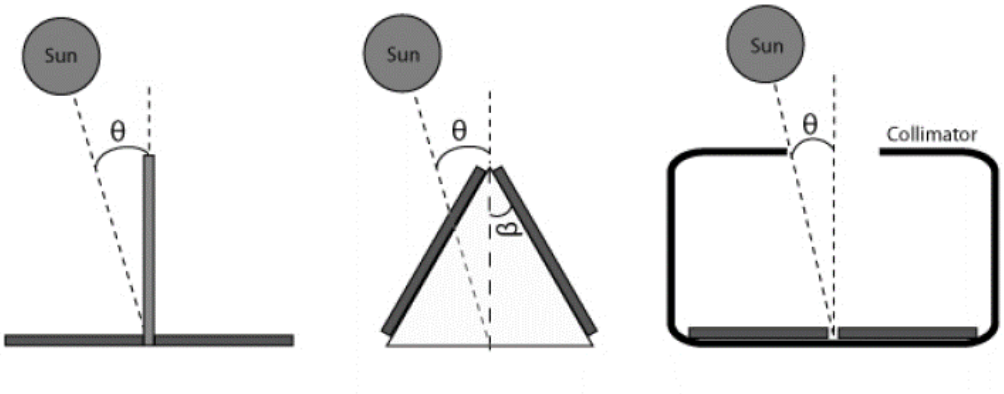

Figure 5. Tracker sensor setups from left to right: Divider, Tilted Mount, and Collimator. (Catarius & Christiner, 2010, p. 8)

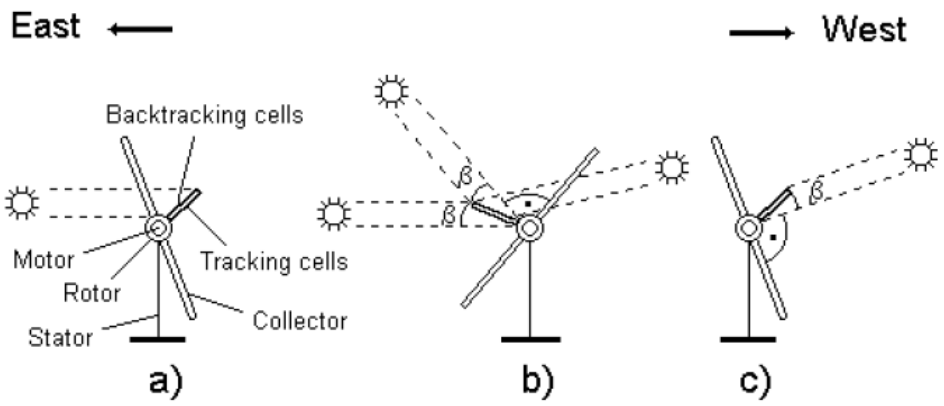

Figure 6. The principle of the auxiliary bifacial solar cell tracker. (Poulek & Libra, n.d., p. 4)

One axis solar trackers can have a horizontal or vertical or inclined rotation axis. Vertical One Axis Solar Trackers (VOASTs) are widely used in regions where the day is long in summertime and the sun is low, compared to Horizontal One Axis Solar Trackers (HOASTs) that are widely used in tropical regions where the sun is high and the day is shorter in summertime. One axis solar trackers are used with PV as well as in parabolic troughs and in linear Fresnel mirror designs. Two axis solar trackers are very important in Concentrated Solar Power (CSP) systems as solar tower systems because of the errors of the angles due to the long distances between the heliostats and the receiver in the tower structure, and in solar dishes (Sterling engines). Two axis solar trackers are used as well in many applications of Concentrated Photovoltaic (CPV) systems to always maintain correct reflection geometry (Rockwell Automation, 2009).

Solar Tracking Algorithms

Michalsky (1988) developed an algorithm that calculates the solar position. That algorithm stated and partially demonstrated accuracy of 0.01^{O} beginning from the year 1950 and applicable until the year 2050. “The algorithm is taken from *The Astronomical Almanac*, which has published it as an addendum to their very accurate tabulations since 1984. It uses

the same approach as an earlier paper by Walvern, but has a more simplified form" (Michalsky, 1988, p. 227). Walvern compared the declination angle in many commonly used algorithms as well. The declination angle is defined as "the angle between the line joining the centers of the sun and the earth and its projection on the equatorial plane" (Mousazadeh et al., 2009, p. 1801). It was shown from this comparison that the *Almanac* algorithm (AA) was the best of the simple algorithms that calculate solar position. "It is superior to the calculations based on least square fits to a given set of data since it is based on the long-term progression of the sun in the ecliptic plane" (Michalsky, 1988, p. 234). "It uses the same approach as an earlier paper by Walraven, but has a simplified form." (Michalsky, 1988, p. 227)

Reda and Andreas (2003) implemented a Solar Position Algorithm (SPA) to calculate the solar zenith and azimuth angles in the period from the year -2000 to 6000, with uncertainties of +/- 0.0003^{O}. Their approach was developed from the book of "Astronomical Algorithms" of Meeus (Reda & Andreas, 2003, p. 16). The solar zenith angle is "a vertical angle between sun's rays and a line perpendicular to the horizontal plane through the point ($\theta_z = 90 - \alpha$)" (Mousazadeh et al., 2009, p. 1801). It is also defined as "the angle between the vertical and a ray from the sun (i.e., the incidence angle for a horizontal surface)" (Braun & Mitchell, 1983, p. 439). In addition, Reda and Andreas introduced some changes to accommodate for solar radiation applications, such as the direction of measuring azimuth angles to be measured from north and eastward, and the direction of measuring the observer's geographical longitude to be measured as positive eastward from Greenwich meridian instead of negative. Reda and Andreas (2003) compared the SPA with the AA of Michalsky. It was shown that the maximum difference between the AA and SPA main parameters is -0.00015^{O}, and the maximum differences between the AA and SPA for calculating the zenith and azimuth angles are $0.00003^{O}$and 0.00008^{O} respectively.

"A key component of the motion controller of trackers is the software, where flexibility, easy-of-use, and integration with other I/O ports are parameters for consideration" (Oh et al., 2009, p. 1). Software like the Laboratory Virtual Instrumentation Engineering Workbench (LabVIEW) was demonstrated by Oh et al. (2009). LabVIEW was used to run the AA tracking algorithm for a modeled two axis azimuth/altitude solar tracking system application. In addition, it was used for developing the application program by calculating the solar azimuth angle, the solar altitude angle, and the times of sunrise and sunset, and by determining the motor steps to send them to the controller. The controller is the device responsible for sending the relevant steps to the motors for the purpose of driving and positioning the tracker towards the sun. In order to determine the accuracy of the calculated angles, the changes in the solar altitude and solar azimuth angles were compared with the results of Korea Astronomy and Space Science Institute (KASI). It was found that the maximum error of the solar altitude angle of the algorithm developed was 0.0371° and the minimum error was 0.0006°. It was also found that the maximum error of the solar azimuth angle of the developed algorithm was 0.0823° and the minimum error was 0.0012° (Oh et al., 2009).

Peterson, Rice, and Vane (2005) described a simpler algorithm based control scheme for the two axis tracker they used. "We decided we wanted to build a two axis solar tracker and start with a basic tracking function and then progressively try and make it smarter and efficient the best we could" (*Introduction* section). Their tracker was powered by Nema 23 bipolar stepper motors to rotate two photovoltaic cells around the altitude and azimuth axes. They used tracking algorithms based on simple tracking functions. The first algorithm was TrackE, which stands for Elementary tracking. The second one was TrackD, which stands for Derivative tracking. The third one was TrackC, which stands for Track Cool. TrackC is the

best algorithm that Peterson et al. (2005) came up with. The first algorithm moves the solar tracker to find the point of highest voltage that satisfies incidence angle $\Theta = 0^{O}$. The second one uses the gradient method, which is calculating the angle Θ required from the tracker to travel in order to achieve the Maximum Power Point (MPP) by knowing three voltages, V_1, V_2, and a reference voltage V, which is already known from the manuals of the solar panels held by the trackers. The third voltage uses the second one to determine five points of sun positions every hour and it predicts the other sun positions over the rest of the hour by using the least square curve fitting method. The minimum errors in altitude and azimuth angles were 0.0562^{O} and 0.3411^{O}, respectively. The maximum errors in altitude and azimuth angles were 1.1294^{O} and 1.6888^{O}, respectively.

Energy Generation Enhancement Due to Solar Tracking

PV systems without tracking mechanisms are simple and have lower initial investment costs but they produce lower power and less energy. The use of tracking systems can boost the collected energy from the sun by 10% to 100% at different times of the year and under different geographical conditions. It is not recommended to use solar trackers with small PV arrays because of the energy consumption of the driving systems, which vary from 2% to 3% of the energy increase delivered by the solar trackers (Mousazadeh et al., 2009; Oh et al., 2009; Patil, Nayak, & Sundersingh, 1997).

A two axis equatorial based tracking mechanism with computer control was designed and fabricated by Patil et al. (1997). The mechanism was tested for several days. The team tested the accuracy of their tracker using a shadow method to measure tracking error. A deviation of only 3^{o} was found throughout the day, and the system yielded a 30% increase in power output compared to a stationary PV module, with only a small amount of power consumed by the tracking motion (Patil et al., 1997).

A novel low cost solar tracker suitable for use in equatorial regions around the world was presented by Clifford and Eastwood (2004). The passive solar tracker was activated by aluminum/steel bimetallic strips and controlled by a viscous damper. The materials and the manufacturing processes used could be done in the developing world, and replicated and maintained in many regions all over the globe. The energy output of the tracking PV panel was 23% more than a typical fixed PV panel.

An interesting design to investigate mechatronics applications to solar tracking systems was done at the College of Technology Directed Projects at Purdue University by Rodriguez (2011). The prototype was a two axis active tilt and azimuth solar tracker. It used two 12-volt DC motors to do the yaw and tilt motions and was controlled by means of three cadmium sulfide photo-resistors. The results showed a 28% increase in the solar energy compared to a stationary panel. “Equipment for this experiment include two solar panels of equal size and output ratings, three equal sets of nickel metal hydride cells, and a real-time prototype solar tracking array” (Rodriguez, 2011, p. 20-21). The three photo-resistors were distributed in the back of the panel array; two were at the top right and left, and one in the middle of the bottom. The reason for that distribution was to create a large difference between the top and the bottom voltages.

A novel PC-based one axis sun tracking system was designed and introduced by Sefa, Demirtas, and Colak (2009). The energy collected from the tracking system was compared with a fixed solar system for the same solar panel. System parameters such as current, voltage, and panel position were observed as well by means of a microcontroller. The tracking system produced 45% more energy than the fixed system (Sefa et al., 2009).

A theoretical model was developed by Helwa et al. (2000) to calculate the hourly solar radiation incident on four different tracking systems, including a fixed PV panel facing

south and tilted at 40°, vertical axis tracker tilted at 33°, one tilted axis tracker with rotating axis in the N-S direction oriented by a tilted angle 6° with the horizontal, and a two axis tracker. The model used calculated global radiation on a horizontal system, diffuse radiation on a horizontal system, and normal radiation, using formulas provided by Stine and Harrigan (1985), Baltas, Tortoreli, and Russell (1986), and Iqbal (1983). Then the calculated values were compared with practical data measured from the four systems installed at the test field of the Institute of Solar Energy and Hydrogen Research located in Widderstall, Germany. It was found that the on-site measured annual average solar radiation incident on the vertical axis tracker was 12% more radiation than that incident on the fixed system. In addition, the on-site measured annual average solar radiation incident on the one tilted axis tracker was 1% more radiation than that incident on the fixed system. Moreover, the on-site measured annual average solar radiation incident on the two axis tracker was 25% more radiation than that incident on the fixed system.

A comparison between the performance of a fixed PV panel at altitude 40° and a Zomeworks one axis solar tracker at altitude 30° was done by Robinson and Raichle (2011). They found that for total irradiance greater than 1100 W/m^2 there was a statistically significant power increase with the Zomeworks one-axis tracker compared to a fixed mount system, ranging from 15% at a lower DBF (50%) to 19% for the upper DBF bins (85%) (Robinson & Raichle, 2011). A 15% to 20% power increase for the Zomeworks one-axis solar tracker was found for all total irradiances as well.

Huang et al. (2009) designed and implemented a solar tracking control system using Field Programmable Gate Arrays (FPGA). A FPGA is an integrated circuit designed to be configured by a customer or a designer after manufacturing. FPGAs are very interesting at

the current time, first of all because they have many logic gates and Random Access Memory (RAM) blocks to do complex digital computations, and second because they accomplish fast integrated operations using bi-directional data buses. The solar tracker was an active two axis azimuth/elevation solar tracker. Cadmium Sulfide (CdS) photo-resistors were used to control the active yaw and tilt motions. An Analog to Digital (A/D) converter was used to deliver the feedback signals to a Cyclone II chip manufactured by the Altera Company in Southern Taiwan. Then an experiment was conducted on the roof of a building at Yuan Ze University to compare the solar tracking system and the fixed panel system. As with other studies, these researchers found the tracking system performed better than the fixed system (Huang et al., 2009). In the mornings and afternoons, the solar tracking system outperformed the fixed system. At 9:30 am, the solar tracking system generated 32.5 KJ while the fixed system generates 25 KJ.At 2:30 pm, the solar tracking system generated 33 KJ while the fixed system generated 24 KJ. The minimum difference between the energy generated in both systems occurs around noon.

In all reported studies except Robinson and Raichle, enhanced energy production was reported under ideal, sunny conditions.

Solar Tracking Error and Accuracy

Looking only at the electrical power generated by a PV array is not enough to determine tracking accuracy because the power output is not just a function of the accuracy. Moreover, the lack of standards that describe tracker performance makes it difficult to evaluate the performance of a solar tracker and therefore it's difficult to compare the performance of various solar trackers. Further, studies undertaken at different locations and times of the year provide performance data under a range of conditions. "These challenges call for a method for accurately characterizing both absolute and relative tracking accuracy in

the field, under a variety of weather conditions" (Stafford, Davis, Chambers, Martinez, & Sanchez, 2009, *Overview* section).

In a patent application publication (U.S. Patent Application No. 18518, 2010), Mark McDonald used a system of two axis (azimuth/elevation) solar trackers carrying a solar collector array. He used a PC-based control system that processes a program code and this program code is connected to a GPS receiver. McDonald claimed "some aspects include determination of a servo feedback signal based on the determined power" and he continued, "determination of the solar tracking error may further include determination of the solar tracking error based on the servo feedback signal and on a relationship between a response of the solar collector and tracking error" (McDonald, 2010, *Abstract* section). He determined the solar tracking error of the solar collector by determining the differences between the power of a servo feedback signals. He reached the conclusion that the solar collector responds late by 0.5°, and that the servo feedback signal corrects the solar collector array position by 2.65°.

Wind Effects on Solar Trackers

Stafford et al. (2009) studied wind velocity and wind direction effects on solar tracking accuracy. Their experiment was done on a commercial CPV. They claimed that the average wind velocity could be misleading. Figure 7 shows the wind velocity as a function of wind direction for the data collected over two months in Puertollano, Spain. The highest wind velocity occurred when the wind direction was towards the east. Because the wind drag force is a function of wind velocity and the orientation of the PV array, the wind drag forces are the highest when the wind direction is out of east, as shown in Figure 8. Figure 9 shows the tracking error versus wind loading. "In considering the effect of wind on trackers, it is

necessary to take into account the changing orientation of the tracker" (Stafford et al., 2009, *Wind loading* section, para. 2). This is important because at certain wind directions and velocities, with certain orientations of the tracker, wind forces may exert external torques on the tracker that affect its motion (especially passive solar trackers), or may increase the load on the fixation of the tracker. The dashed line in Figure 9 shows 0.76^{O} median tracking error caused by wind loading.

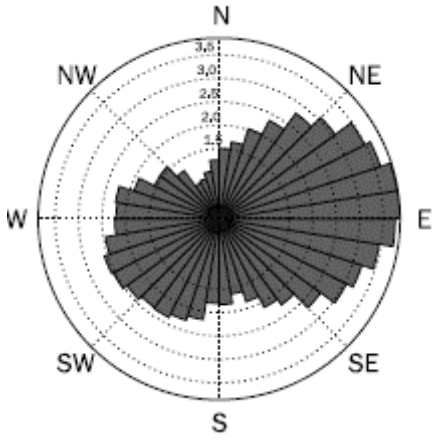

Figure 7. Average wind velocity [m/s] vs. direction (Stafford et al., 2009, Figure 2).

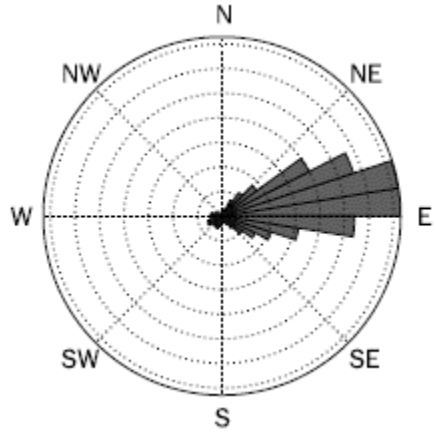

Figure 8. Drag force [% of max] vs. direction (Stafford et al., 2009, Figure 3).

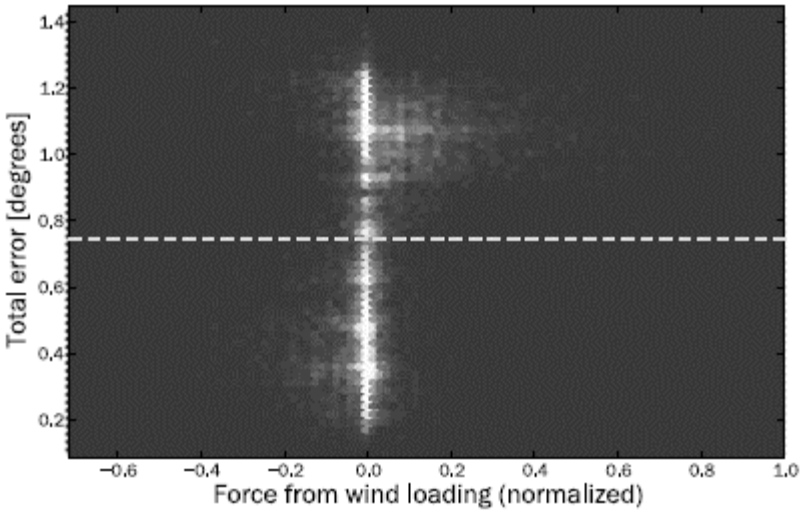

Figure 9. Tracking error caused by wind loading (Stafford et al., 2009, Figure 5). Notice the line of light indicates the different tracking errors at zero wind loading. Notice also that positive wind loading results in large tracking error while negative wind loading results in low tracking errors.

CHAPTER 3: RESEARCH METHODOLOGY

Overview of Research Design

This experiment measured the elevation angle and the azimuth angle of a non-algorithm based two axis solar tracker and the azimuth angle of the non-algorithm based passive one axis solar tracker in the Appalachian State University Solar Research laboratory. These angles were then compared to the angles calculated by Michalsky's celestial algorithm. From this comparison, the accuracy of tracking of these two types of solar trackers was determined.

Experimental Design

The vision behind this study was to add another pillar to the performance comparison of the solar trackers besides their power generation, namely, their ability to accurately point to the sun. By carrying out this study a residential owner could be able to make a better decision about whether to install a fixed panel, one axis tracker, two axis tracker, or even no PV system at a certain site based on a complete study of performance of the systems. This study was begun in January, 2012. The objective was to measure the angles of the one axis and two axis solar trackers located at the Solar Research lab and to compare the actual angles with algorithmic calculated angles to determine the trackers' accuracy in following the sun's path. Different potentiometers were mounted on the solar trackers and calibrated to measure the actual angles of the trackers.

Site Characteristics

Figure 10. Large dense area of high woods behind the ASU Solar Research lab causing shading.

Figure 11. Trees and lights in front of the lab causing shading.

Figure 10 shows the Appalachian State University Solar Research Facility Laboratory. The lab is located at the University's State Farm Complex in Boone, North Carolina. The latitude and the longitude of the site are 36.2167^{O}N and 81.6747^{O}, respectively. The true north, south, east, and west directions are shown in Figure 12. There is a flat open area between true north and 45^{O} west of true south as shown in Figure 12. Figure 12 also shows that there is a small house and dense area of woods with high trees from 45^{O} west of true south to true north. Those woods are behind the Solar Lab, as shown in Figure 10. The small house and the woods behind the lab cause shading for the one axis and two axis solar trackers located in the lab. Figure 12 shows trees located in front of the lab from 135^{O} east of true south to 45^{O} west of true south. Those trees cause shading for the pyrheliometer which measures DNI. Figure 12 shows that shading effects take place from 45^{O} west of true north to 45^{O} west of true south (in between tilt angles of $0^{O}$and $36^{O}$for the PV array).

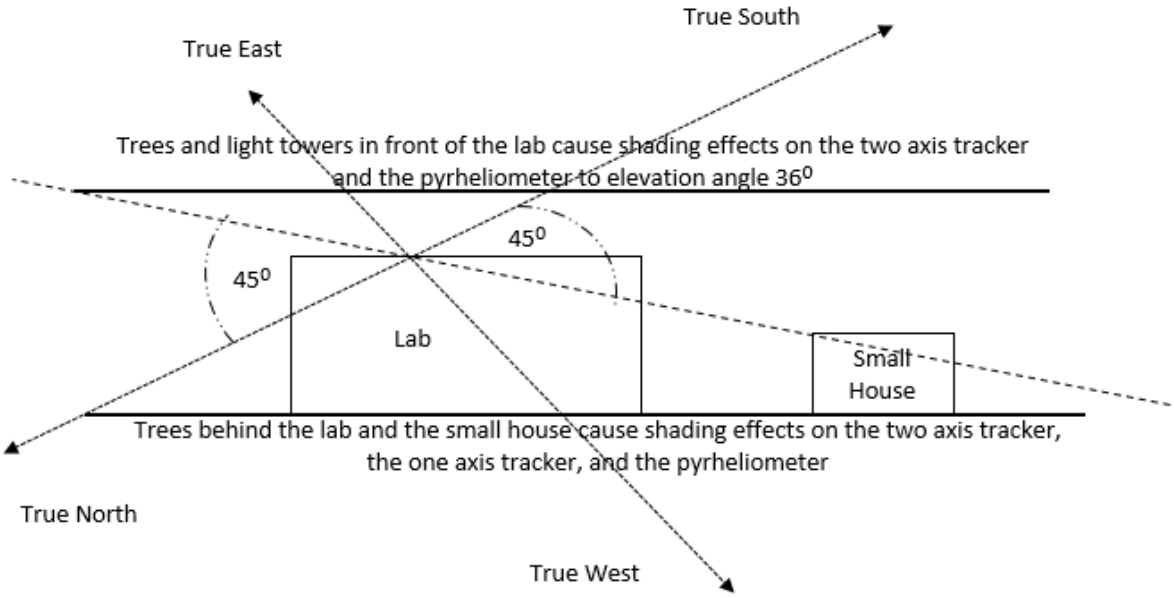

Figure 12. Plan view of the lab showing shading points and angles.

Tracking Motions of the Solar Trackers Used

Zomeworks UTR-020 solar tracker

As shown and explained in materials located in Appendix B, the Zomeworks UTR-020 used in the study doesn't move by either motors or gears. It moves by the difference in weight produced from the thermal expansion of the working fluid in the two canisters of the solar trackers. This is enhanced by aluminum shadow plates surrounding the two canisters of the solar tracker. Zomeworks UTR-020 is a one axis solar tracker.

In the morning, the Zomeworks UTR-020 solar tracker begins its motion from where it stopped at sunset of the previous day. As the sun rises and its rays hit the aluminum shadow plates and the canisters of the solar tracker, the working fluid heats and expands differently in the two canisters of the solar tracker. Hence, the two cylinders contain different weights of fluid and the tracker moves. The solar tracker continues in its motion until balance

occurs when the weights of the working fluid in the two canisters are equal. The balance happens when the sun's rays are normal to the surface of the PV array, where incidence angle θ equals to 0º. This behavior of the Zomeworks UTR-020 takes place throughout the day until sunset.

Wattsun AZ-225 solar tracker

The Wattsun AZ-225 Solar Tracker is a dual axis solar tracker. The two axes of motion are the azimuth and altitude axes. The motion around the azimuth axis is called yaw motion, and the motion around the altitude axis is called tilt motion. The tracker is moved by two motors, which are controlled by two pairs of photo-resistors. The photo-resistors can also be referred to as Light Dependent Resistors (LDRs). An LDR is an electronic component whose resistance decreases with increasing incident light intensity. One pair of LDRs is responsible for the yaw motion of the solar tracker around the azimuth axis. The other pair of LDRs is responsible for the tilt motion of the solar tracker around the altitude axis.

Before the morning, the Wattsun AZ-225 solar tracker is automatically moved from where it stops the previous day at sunset to the east and to its maximum tilt where the sun begins to rise above the horizon. As the sun's rays hit the LDR pairs, different light intensities are produced and so different resistances take place. This causes two electronic signals to be sent to the controller. The first signal is sent from the LDR pair responsible for the yaw motion to the motor. Hence, the motor moves the tracker to the proper azimuth position. The proper azimuth position is where the surface azimuth angle γ equals to solar azimuth angle γ_s. The second signal is sent from the LDR pair responsible for the tilt motion to the motor. Hence, the motor moves the tracker to the proper altitude position. The proper altitude position is where the inclination angle β becomes complementary with the solar

altitude angle α. With these positions, the sun's rays become normal to the surface of the PV array where incidence angle θ equals to 0º. This behavior of the Wattsun AZ-225 takes place throughout the day until sunset.

Instrumentation

Figure 13 shows a block diagram of the experiment. There were three main components of the experiment: the two solar trackers, where the three potentiometers were mounted; the solar and wind meteorological stations and the pyranometer that measured the GHI; and the data logger and its software. The PV panels mounted on each of the two solar trackers were Sharp ND-224UC1 solar panels grid connected with enPhase micro inverters.

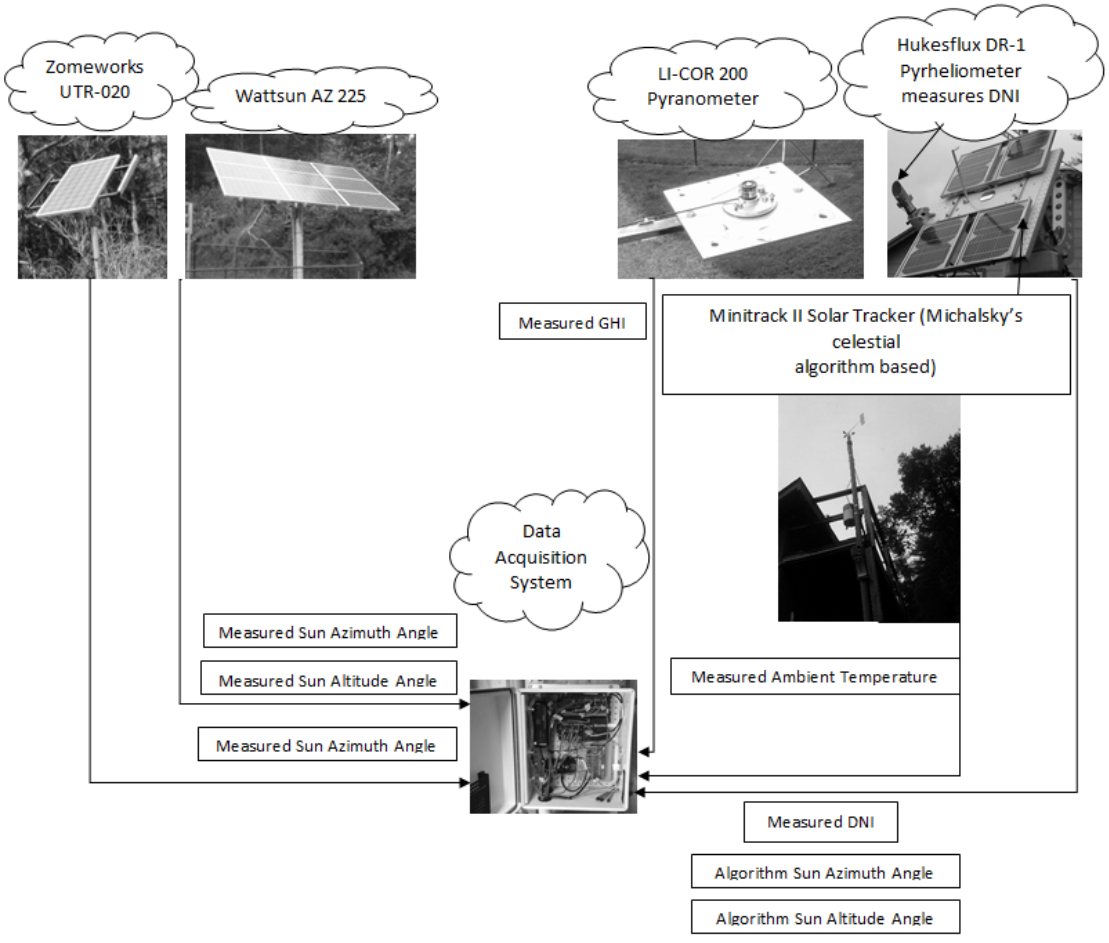

Figure 13. A block diagram of the experiment.

Measurement of azimuth and elevation angles

The azimuth angle of the passive one axis solar tracker was measured by a 6”, 10k linear potentiometer. The azimuth angle of the active two axis solar tracker was measured by means of a 10:1 gear box and a 10-turn, 100k rotating potentiometer mechanically coupled to the azimuth drive assembly. The elevation angle of the active two axis solar tracker was measured by a 900 mm, 100k linear potentiometer. The resistance of each potentiometer was measured using a ½ bridge circuit. Angles were determined from measured resistances based on empirical calibration functions.

Meteorological stations

The DNI was measured by a Hukesflux DR-1 Pyrheliometer (first class) pointed at the sun by a Minitrack II Solar Tracker (Michalsky’s celestial algorithm based). The GHI was measured by a LI-COR 200 Pyranometer. The ambient temperature was measured by a Campbell Scientific HMP 50 temperature and humidity sensor.

Half bridge circuit

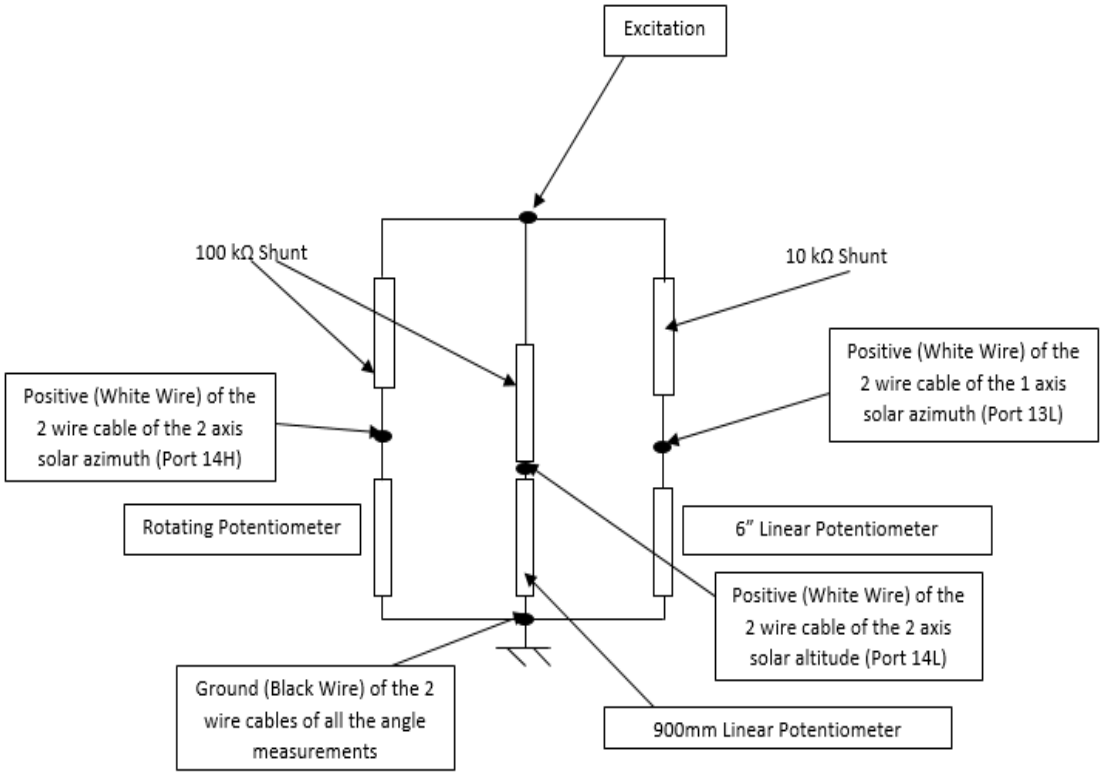

Figure 14. The wiring layout of the half bridge circuits.

The three potentiometers were connected to a CR1000 data logger through half bridge circuits, as shown in Figure 14. The other measuring devices had been already connected before this research started in the lab. Figure 14 shows the wiring layout of the three potentiometers to the data logger. Three two-wire cables were used in the wiring. One 10 kΩ shunt resistor was connected in series with the 6" linear potentiometer. One 100 kΩ shunt resistor was connected in series with the 900 mm linear potentiometer. Another 100 kΩ shunt resistor was connected in series with the 10-turns rotating potentiometer. Each shunt resistor and the corresponding potentiometer connected in series with it are connected in parallel between the excitation voltage and the ground.

Calibration of the Potentiometers

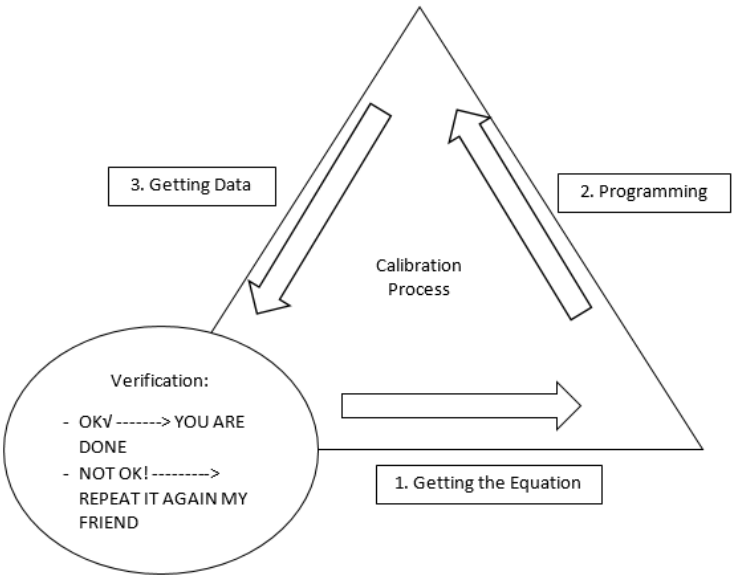

Figure 15. A diagram of the calibration process used in the study.

The objective of the calibration process was to get the angle/resistance transfer function of each of the potentiometers. Each tracker in turn was manually positioned at a known angle and its output recorded. Each equation was determined by choosing the best curve fit to an angle vs. output graph of each potentiometer. The software used in this was Microsoft Excel. After the equation of each measurement had been determined, the equation was compiled to LoggerNet software, which is the software used in the Data Acquisition System of the Solar Research lab. The verification process compared the curves of the sun angles calculated from the algorithm and the measured angles on a very sunny day. This process took place for each of the three potentiometers individually.

Calibration of the 6” linear potentiometer

The idea of mounting a 6” linear potentiometer on the non-algorithm based passive one axis solar tracker came from the occurrence of relative sliding motion between

components of the damper, as shown in Figure 16. The maximum distance traveled through this motion is 6". The calibration was done in order to get a relation between the output of the 6" linear potentiometer and the actual azimuth angle of the tracker. The output of the 6" linear potentiometer mounted was "$V_{potentiometer}/V_{excitation}$", where $V_{excitation}$ was 2500 mV for the potentiometer used. The relation between output of the 6" linear potentiometer and the azimuth angle of the passive one axis solar tracker is shown in Figure 17, through which the best fit calibration equation is the quadratic equation shown in Equation 1. From Figure 17, the sensitivity of the 6" linear potentiometer is 4.9 mV/degree. Equation 1 shows the calibration equation by which the azimuth angle of the one axis solar tracker was determined. The main sources of uncertainty in this equation is the from determining the tracker angle. The statistical uncertainty is around -/+1˚.

$$Az° = -1591.7\left(\frac{V_{potentiometer}}{V_{excitation}}\right)^2 + 1840.3\left(\frac{V_{potentiometer}}{V_{excitation}}\right) - 296.85 \quad (1)$$

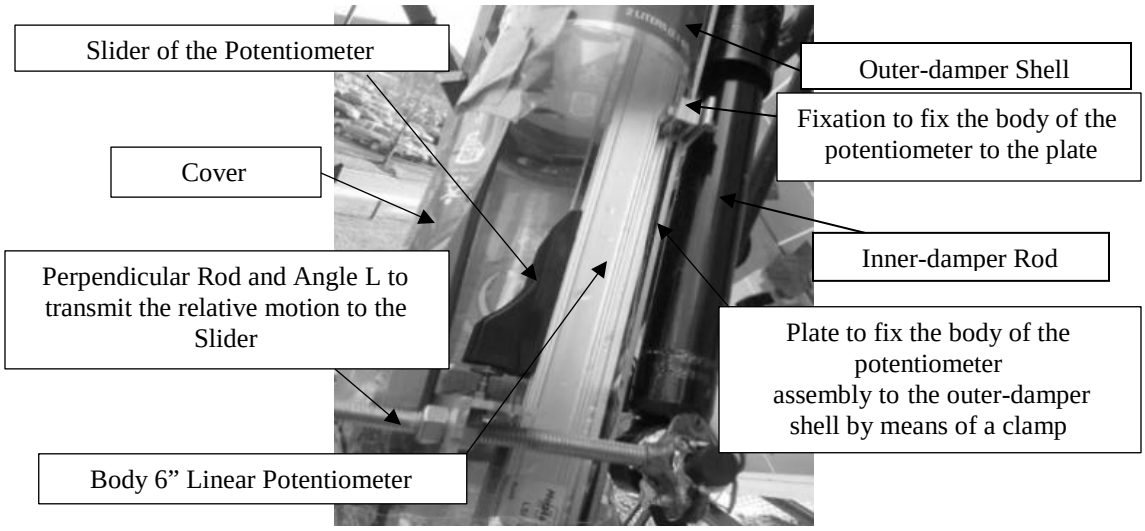

Figure 16. Mounting of the 6" Linear Potentiometer.

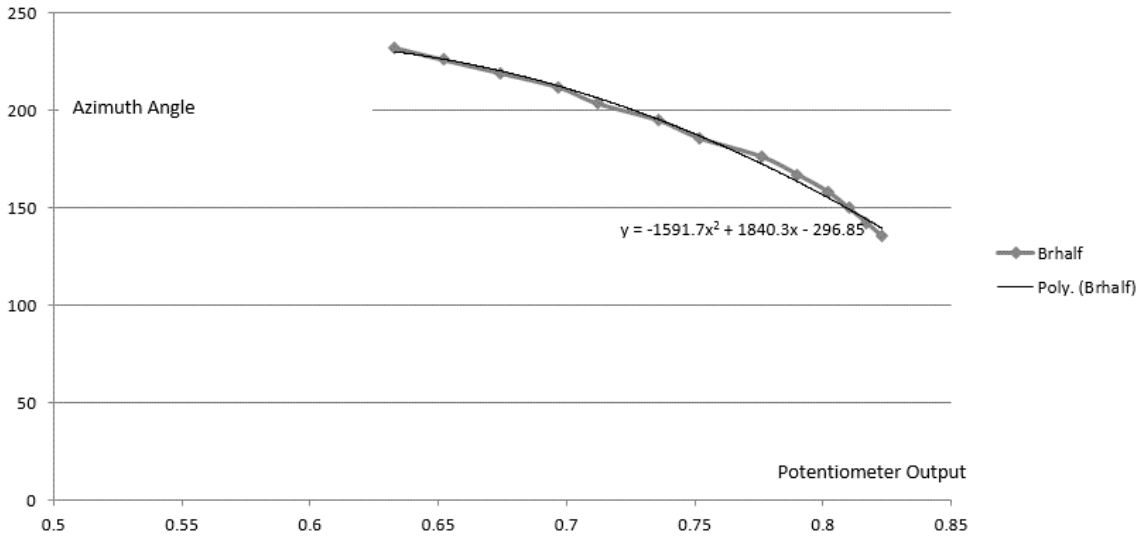

Figure 17. The relation between output of the 6" linear potentiometer and the azimuth angle of the passive one zxis solar tracker.

Calibration of the 10-turns rotating potentiometer

The idea of mounting a five-turns rotating potentiometer on the non-algorithm based active two axis solar tracker came from the occurrence of rotation motion of the Shaft 1 as shown in Figure 18. The calibration was done in order to get a relation between the output of the rotating potentiometer and the actual azimuth angle of the tracker. The output of the rotating potentiometer mounted was "$V_{potentiometer}/V_{excitation}$", where $V_{excitation}$ was 2500 mV for

the potentiometer used. The relation between output of the rotating potentiometer and the azimuth angle of the active two axis solar tracker is shown in Figure 19, through which the best fit calibration equation is the quadratic equation shown in Equation 2. From Figure 19, the sensitivity of the ten-turns rotating potentiometer is 1.5 mV/degree. Equation 2 shows the calibration equation by which the azimuth angle of the two axis solar tracker is determined. The main source of uncertainty in this equation is from determining the tracker angle. The statistical uncertainty is around -/+1˚.

$$Az° = -2409.5\left(\frac{V_{potentiometer}}{V_{excitation}}\right)^2 + 297.19\left(\frac{V_{potentiometer}}{V_{excitation}}\right) + 470.69 \quad (2)$$

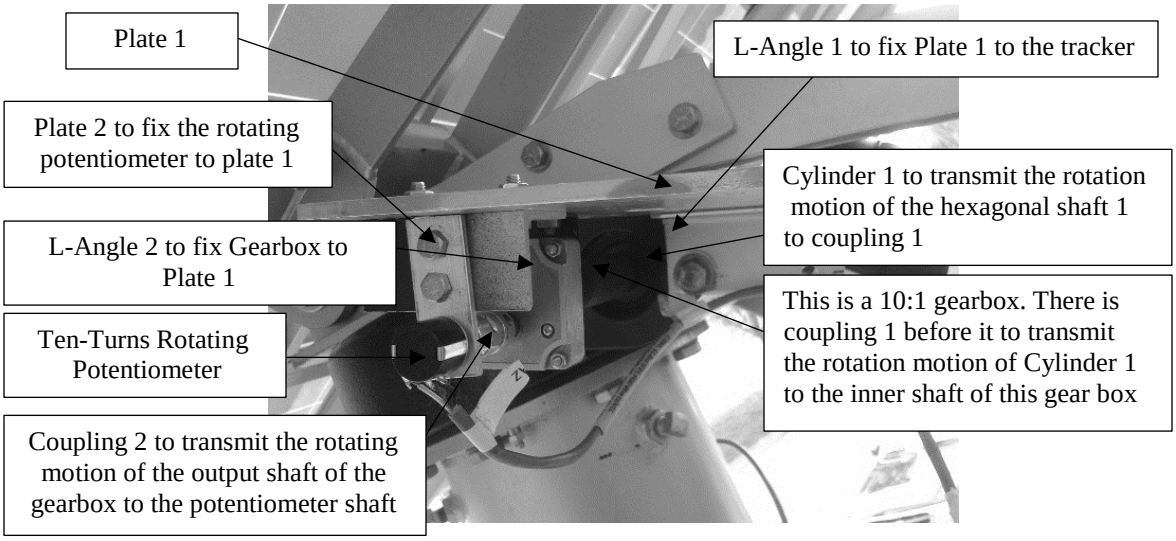

Figure 18. Mounting of the five-turns rotating potentiometer.

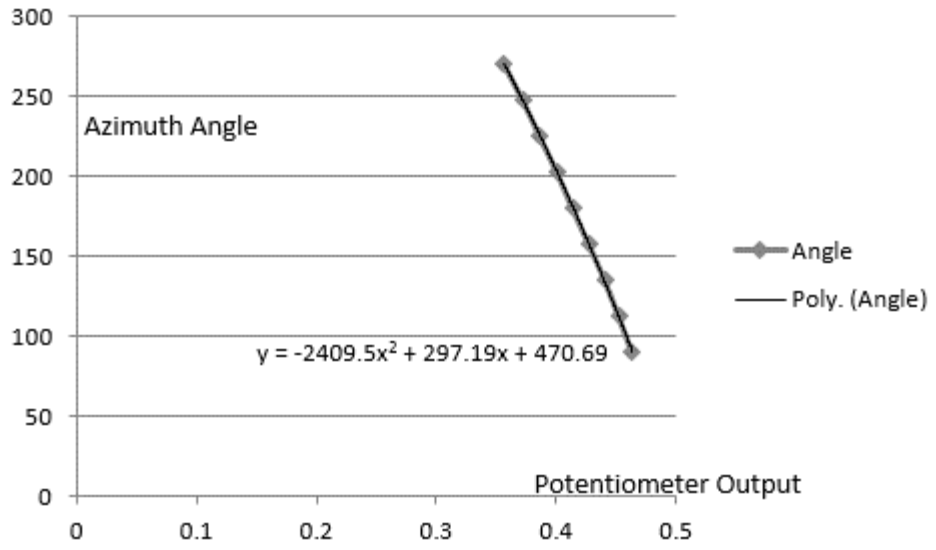

Figure 19. The relation between output of the rotating potentiometer and the azimuth angle of the active two axis solar tracker.

Calibration of the 900 mm linear potentiometer

The idea of mounting a 900mm linear potentiometer on the non-algorithm based active two axis solar tracker came from the occurrence of relative sliding motion between the internal and external shafts connected to the tilt motion motor of the tracker, as shown in Figure 20. The calibration was done in order to get a relation between the output of the 900mm linear potentiometer and the actual elevation angle of the tracker. The output of the 900mm linear potentiometer mounted was "$V_{potentiometer}/V_{excitation}$", where $V_{excitation}$ was 2500 mV for the potentiometer used. The relation between output of the 900mm linear potentiometer and the elevation angle of the active two axis solar tracker is shown in Figure 21, through which the best fit calibration equation is the quadratic equation shown in Equation 3. From Figure 21, the sensitivity of the ten-turns rotating potentiometer is 14.4 mV/degree. Equation 3 shows the calibration equation by which the elevation angle of the two axis solar tracker was determined. The main source of uncertainty in this equation is from determining the tracker angle. The statistical uncertainty is around -/+1˚.

$$Elev° = 281.53\left(\frac{V_{potentiometer}}{V_{excitation}}\right)^2 + 8.4164\left(\frac{V_{potentiometer}}{V_{excitation}}\right) + 6.3035 \quad (3)$$

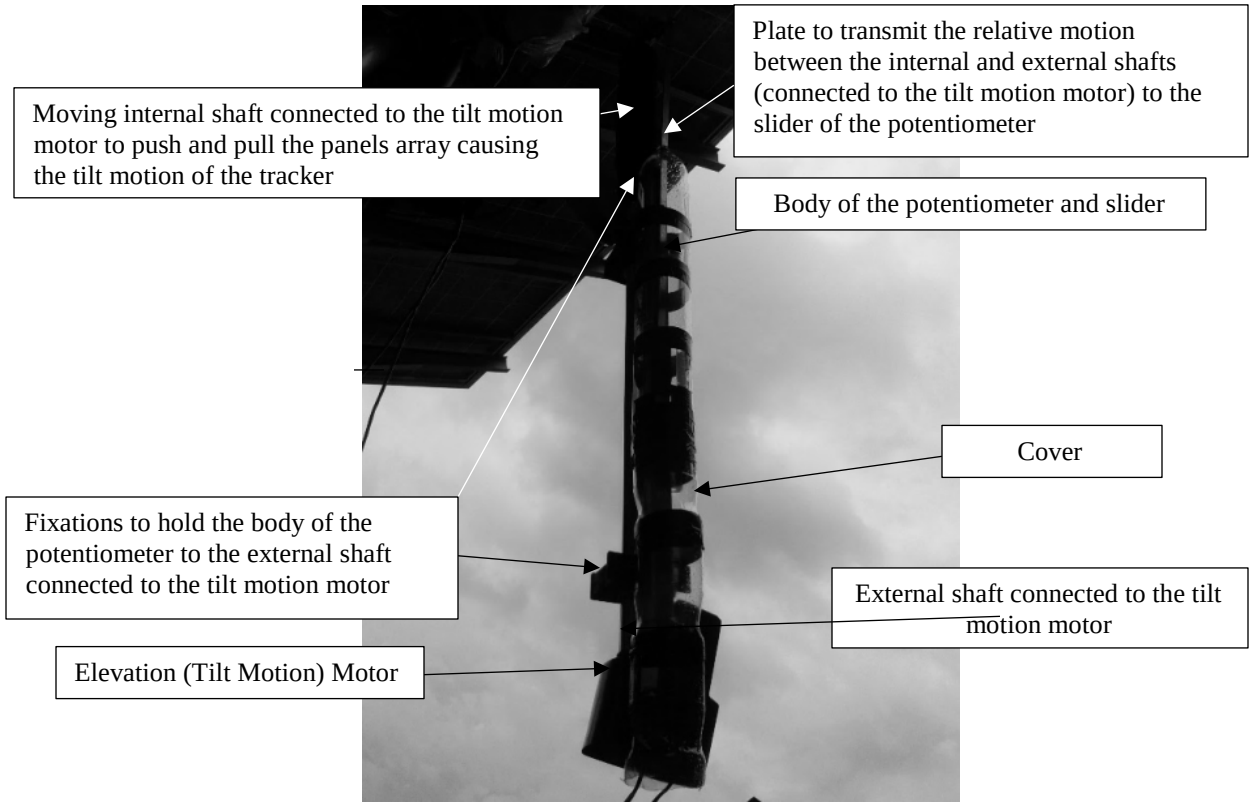

Figure 20. Mounting of the 900mm linear potentiometer.

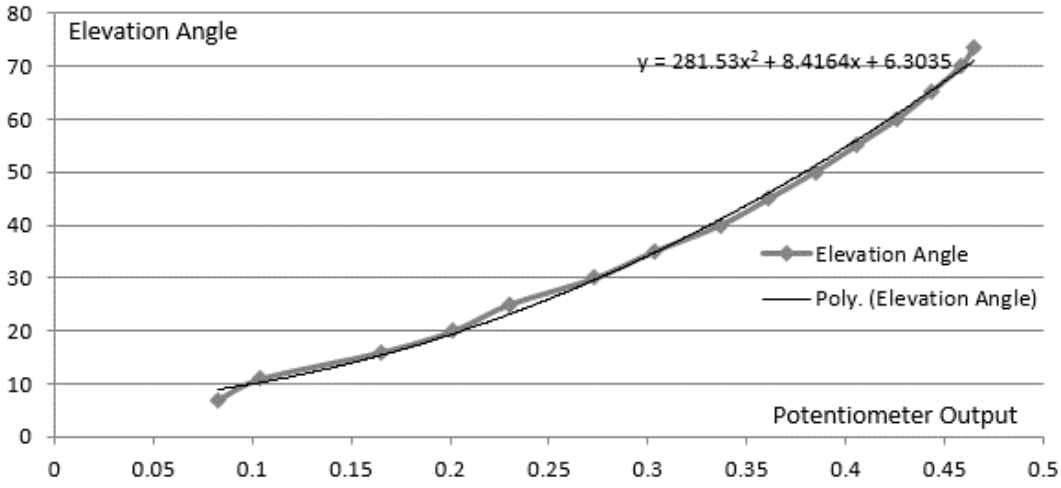

Figure 21. The relation between output of the 900mm linear potentiometer and the elevation angle of the active two axis solar tracker.

Data Collection

Sample

The data sample included one minute averages calculated from a 10-seconds sampling rate of the measured azimuth angles of the passive one axis solar tracker and active two axis solar tracker, the measured elevation angle of the two axis solar tracker, the angles calculated by Michalsky's celestial algorithm, the DNI, the calculated Global Horizontal Irradiance (GHI), the GHI measured in the lab, the wind speed, the wind direction, and the ambient temperature. The data collection period was from February 10th to June 16th, 2013 for the azimuth angle of the Zomeworks UTR-020 passive azimuth solar tracker, and from May 16th to June 16th, 2013 for the other two angles of the Wattsun AZ-250 solar tracker. The raw data included 195,272 minutes for the Zomeworks UTR-020 azimuth solar tracker and 46,081 minutes for the Wattsun AZ-225 solar tracker.

Data Collection Process

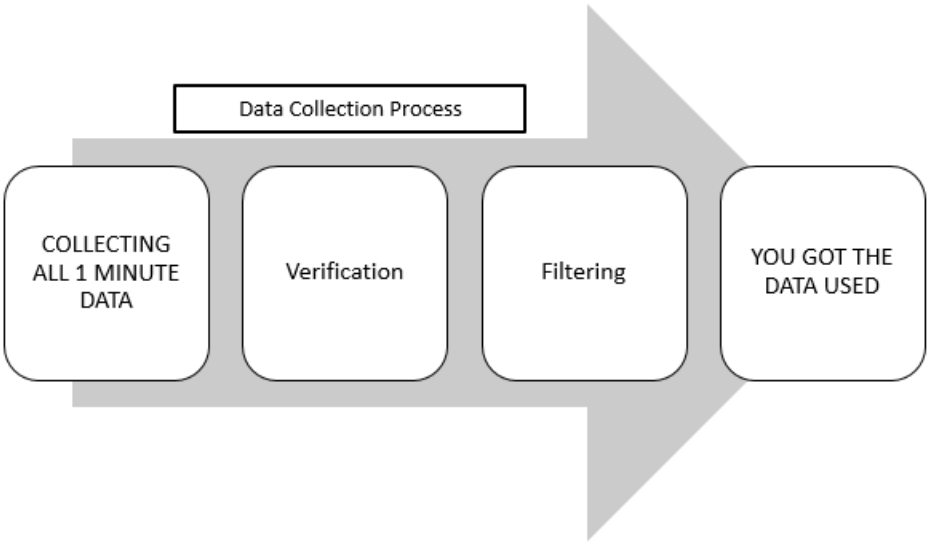

Figure 22. A diagram of the data collection process.

The data collection process consisted of two consecutive stages: the verification process and the filtering process. The input was one minute data in text files format generated by the data acquisition system used. Those files were then converted to Excel files to apply the verification, filtering, and various analysis processes. The verification process was carried out in order to validate the data by assuring that, first, all the data were from sunrise to sunset; second, the measured azimuth and elevation angles were positive; third, the measured azimuth angles were less than or equal to 360^{O}; and fourth, the DBF percentages were positive and less than or equal to 100 %, and by comparing the calculated GHI and the measured GHI so that the calculated GHI was different from the measured GHI by no more than 10%. After that a filtering process took place. The idea for the filtering process was to exclude the data collected of measured GHI less than 100 W/m^2, the data collected while shading affected the solar trackers, and any data that described non-physical performances of the trackers. The reason for this filtering was to reduce sensitivity to low power, high noise conditions and to better generalize the results and conclusions of the study to any location on the globe, because DBF and GHI depend on the climatic conditions in the location of the trackers and change from one place to another. After the verification and filtration processes were executed, the remaining data included 32,405 minutes (17% of total) for the Zomeworks UTR-020 solar tracker and 14,118 minutes (31% of total) for the Wattsun AZ-225 solar tracker.

Data Analysis Procedures

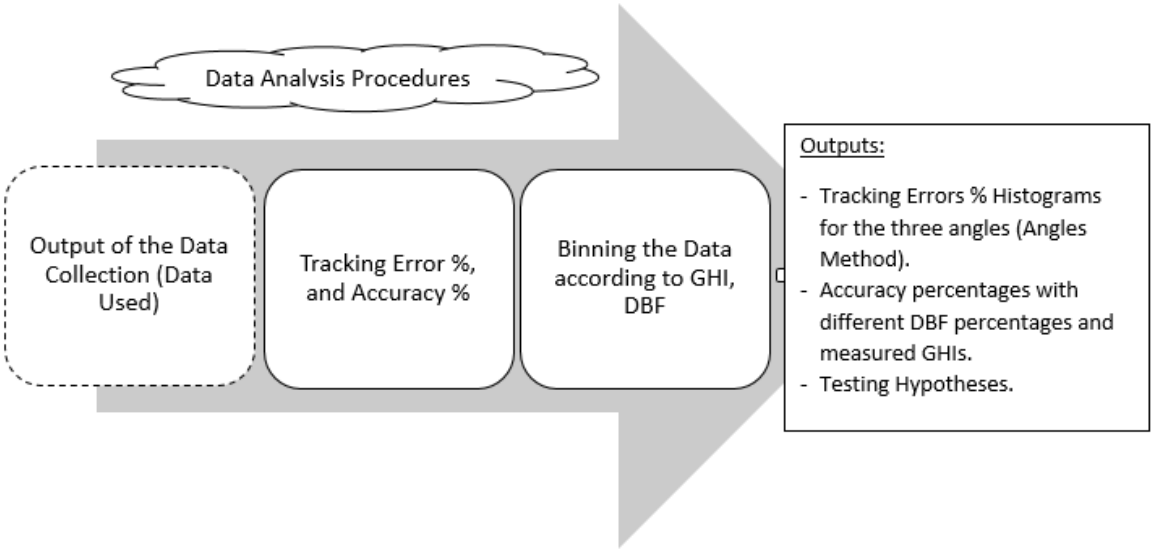

Figure 23. A diagram of the data analysis procedures.

The input for data analysis was the data output from the data collection strategies. The DBF, the Tracking Error %, and the Accuracy % were calculated as shown in Equations 4, 5, and 6, respectively. Hence, tracking error percentage histograms for the three measured angles were determined. This method is called "Angles Method to determine the accuracy of solar trackers." In addition, Hypotheses 1 & 3 were tested by calculating the correlations of accuracies of the measured angles with DBFs and ambient temperatures. The following equations show how to determine the Direct Beam Fraction (DBF), the tracking error percentage, the accuracy percentage, and the correlation between two variables, respectively.

$$DBF = \frac{DNI * \sin \alpha}{GHI_{meas.}} \tag{4}$$

where,

DBF: Direct Beam Fraction.

DNI: Direct Normal Irradiance.

α: Sun Elevation Angle.

$GHI_{meas.}$: Global Horizontal Irradiance.

$$Tracking\ Error\ \% = \frac{(Angle_{meas.} - Angle_{calc.}) * 100}{Angle_{calc.}} \quad (5)$$

where,

$Angle_{meas.}$: Angle measured from the potentiometers.

$Angle_{calc.}$: Angle calculated by Michalsky's celestial algorithm.

$$Accuracy\ \% = \ 100 - |Tracking\ Error\ \%| \quad (6)$$

$$r = \frac{1}{n-1} \sum (\frac{x_i - \overline{x}}{s_x}) (\frac{y_i - \overline{y}}{s_y}) \quad (7)$$

where,

r: Correlation.

n: Sample size.

x_i, and y_i: The two targeted variables.

$\overline{x}$, and $\overline{y}$: The sample means of the two targeted variables.

s_x, and s_y: The standard deviations of the two targeted variables.

After those calculations were performed, the data were organized in different categories of DBFs and measured GHIs. The reason for having these different categories was to analyze the data in different clear and cloudy weather conditions. In this way the research question was answered and Hypothesis 2 was tested when accuracies via weighted averages were calculated for the different categories of DBFs and measured GHIs.

CHAPTER 4: RESEARCH FINDINGS

Representation of Angles with Time on a Sunny Day

In the data analysis, a graphical representation of the collector and sun angles on a sunny day is shown in order to understand the behavior of the azimuth angles of both the Zomeworks UTR-020 passive azimuth solar tracker and the Wattsun AZ-225 active azimuth elevation solar tracker with time of the day. Another graphical representation was created to understand the behavior of the elevation angle of the Wattsun AZ-225 active azimuth elevation solar tracker throughout the day as well.

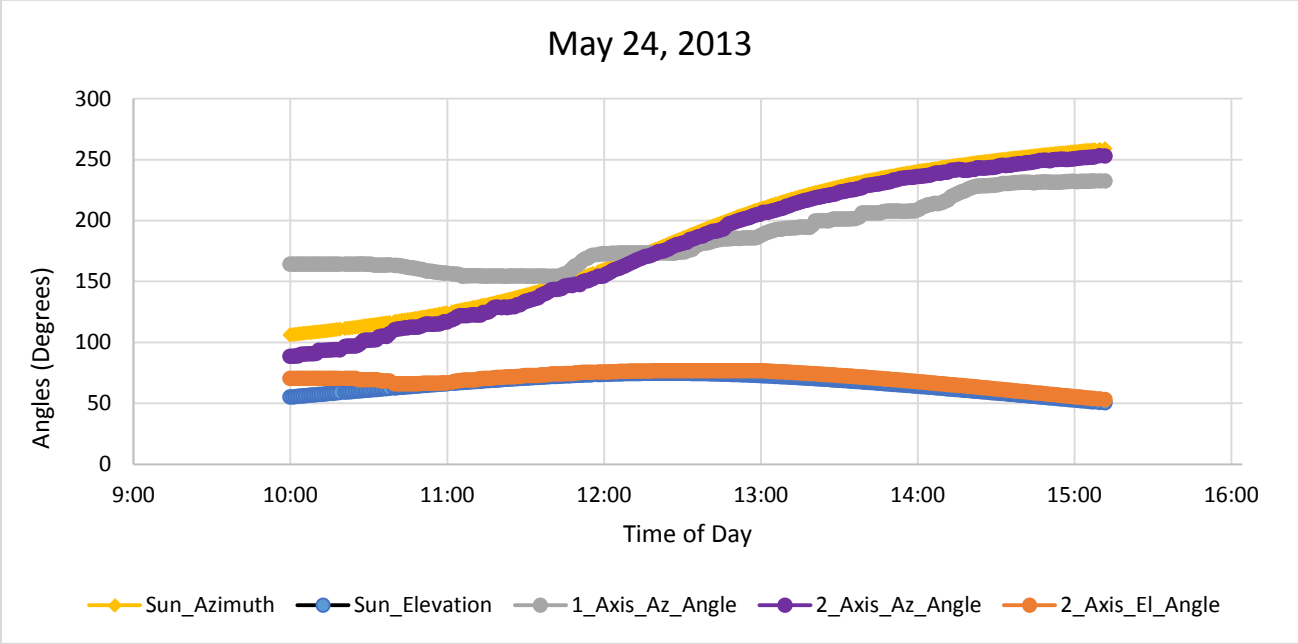

Figure 24. Angles on a sunny day (May 24, 2013).

Figure 24 shows the behavior of the collector and sun angles in degrees according to the local standard time. It shows the angles from 10:00 am to 3:00 pm on May 24, 2013, a

day selected from the filtered data because it was a sunny day. The sun azimuth and the sun elevation angles shown are the angles that were calculated by the celestial algorithm of Michalsky (1988). The 1_Axis_Az_Angle is the azimuth angle of the Zomeworks UTR-020 passive azimuth solar tracker. The 2_Axis_Az_Angle is the azimuth angle of the Wattsun AZ-225 active azimuth elevation solar tracker. The 2_Axis_El_Angle is the elevation angle of the Wattsun solar tracker as well. The differences between the sun azimuth angle and the Wattsun two axis azimuth angle are very small, and they represent the low tracking errors and the high accuracy of the azimuth angle of the Wattsun solar tracker used in the experiment. Small differences are also shown between the sun elevation angle and the Wattsun two axis elevation angle. These differences represent the low tracking errors and the high accuracy of the elevation angle of the Wattsun solar tracker used in the experiment. The errors are primarily present in the morning hours.

It is clear from Figure 24 that there are big differences between the azimuth angles of the sun and of the Zomeworks passive solar tracker used in the experiment, which represent higher tracking errors and lower accuracies of the Zomeworks tracker. In addition, Figure 26 shows that these differences decreased until 12:19 pm, after which they increased. The azimuth angle of the Zomeworks tracker was more than the sun azimuth angle in the morning with maximum difference in the early morning. This difference decreased until it equaled zero before it increased again. Moreover, the azimuth angle of the Zomeworks passive solar tracker became less than the sun azimuth angle when the differences between the angles increased again. This behavior shown for the Zomeworks passive solar tracker appeared to be consistent with its passive method of tracking motion to follow the sun as explained in Chapter 3 (Tracking Motions of the Solar Trackers Used section). In the early morning, the tracker was still looking to the west where it was positioned as the sun set on the previous

day, and so the torque needed to rotate the tracker is greatest. In addition, the early morning radiation is weak, resulting in a small differential expansion of the tracker's working fluid and a small rotation torque. Consequently, the tracker tends to miss the sun in the very early morning.

Tracking Error Histograms

One Axis Zomeworks UTR-020 Azimuth Angle

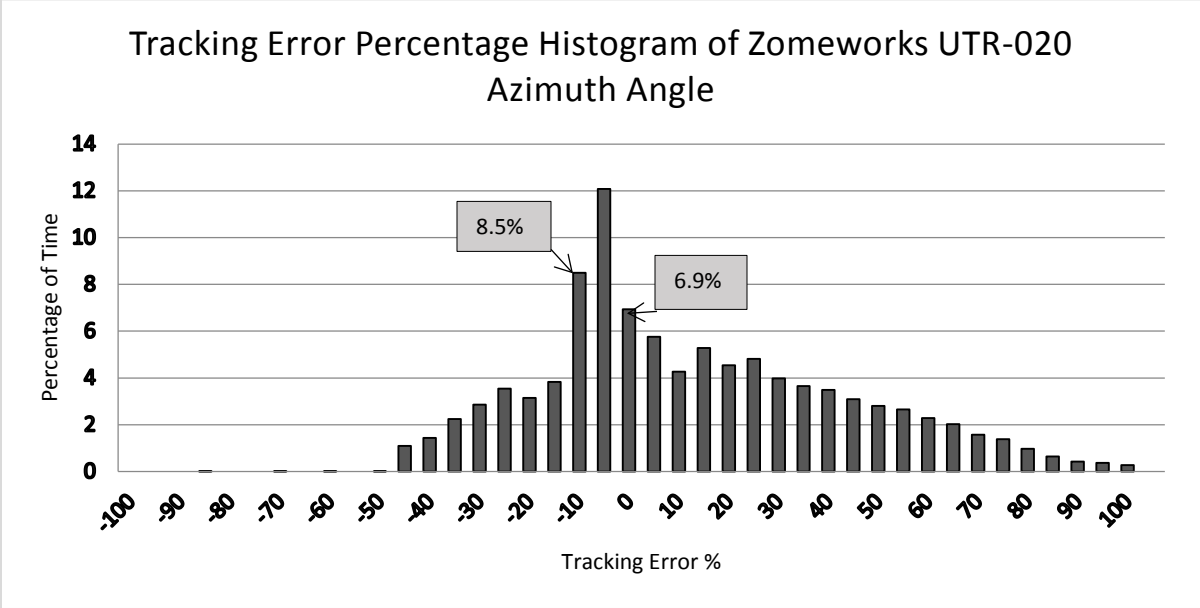

Figure 25. Tracking error percentage histogram of Zomeworks UTR-020 azimuth angle.

Figure 25 shows the histogram of the tracking errors of the azimuth angle of the Zomeworks solar tracker used in the experiment. The histogram is generally normally distributed with a large standard deviation but skewed to the right and with an average tracking error +25% and median tracking error +19% with dominant mode at 5% tracking error. The behavior of the Zomeworks solar tracker looking to the west in the morning of each day (as explained in the previous section) explains the large positive tracking errors shown in the histogram of Figure 25. The one mode of -5% tracking error shows that the tracker spends 12% of the time behind the sun by 5% after catching it around noon. The

tracker spends 8.5% of the time with -10% tracking error. The tracker spends 6.9% of the time with 0% tracking error. Zero percentage tracking error means that the tracker points exactly towards the sun and the incidence angle equals to 0° where all the conditions of the optimum solar tracker orientation explained in Chapter 2 (Solar Tracking Geometry section) apply.

Two Axis (Wattsun AZ-225) Azimuth Angle

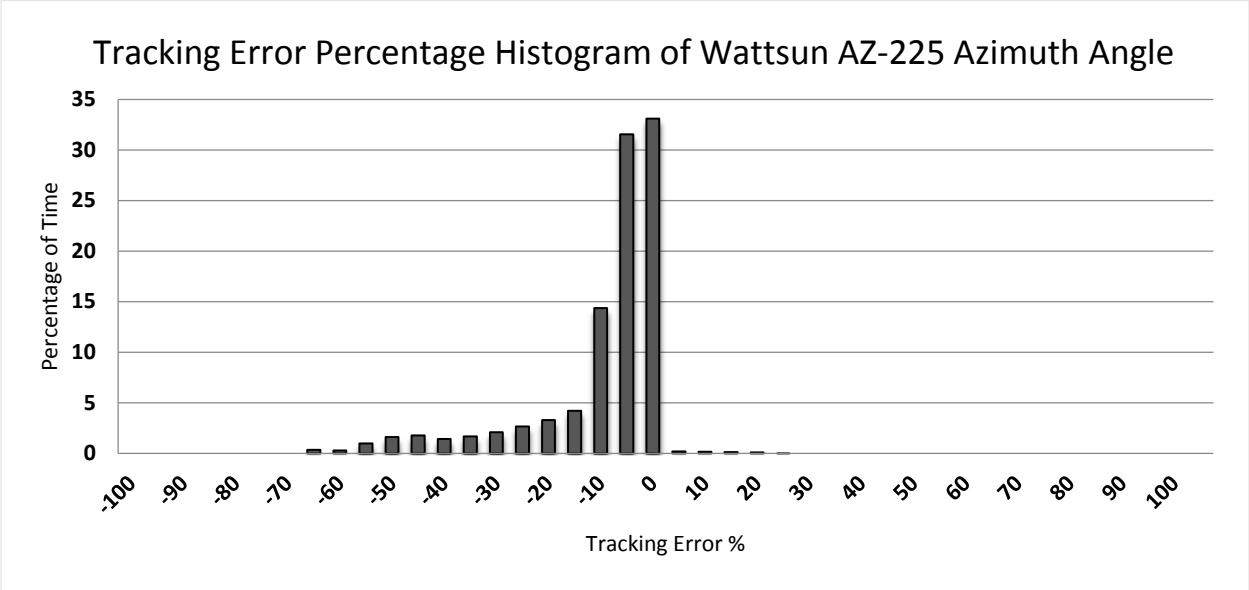

Figure 26. Tracking error percentage histogram of Wattsun AZ-225 azimuth angle.

Figure 26 shows the histogram of the tracking errors of the azimuth angle of the Wattsun solar tracker used in the experiment. The histogram generally follows a normal distribution with a relatively small standard deviation but is skewed to the left with an average tracking error of -12% and median tracking error of -7% with one mode of 0% tracking error during 33.1% of the time. Azimuth tracking rarely leads the sun azimuth position, but lags the sun azimuth angle by more than 10% around 15% of the time. Zero percentage tracking error means that the tracker points exactly towards the sun and the

incidence angle equals to 0° where all the conditions of the optimum solar tracker orientation apply.

Two Axis (Wattsun AZ-225) Elevation Angle

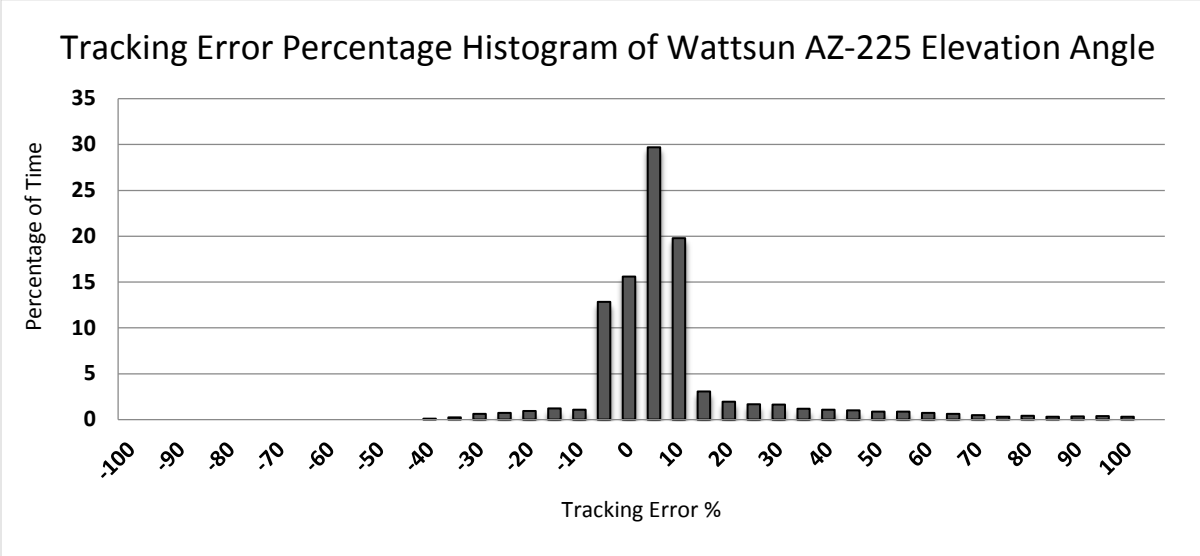

Figure 27. Tracking error percentage histogram of Wattsun AZ-225 elevation angle.

Figure 27 shows the histogram of the tracking errors of the elevation angle of the Wattsun solar tracker used in the experiment. The histogram is generally normally distributed with a relatively small standard deviation with an average tracking error of +11% and median tracking error of +6% with one mode of +5% tracking error. Elevation tracking seems to over- and under-shoot the sun position by greater than 10% with approximately equal frequency – less than 10% of the time in each case. In addition, gross overshooting is occasionally experienced. The one mode at +5% tracking error shows that the tracker spends 29.7% of the time pointing exactly towards the sun and the incidence angle equals to 0° where all the conditions of the optimum solar tracker orientation apply.

CHAPTER 5: CONCLUSIONS AND DISCUSSION

Research Question Conclusions

This research was guided by one primary research question:

RQ1: What is the accuracy of non-algorithm based one-axis solar trackers and two-axis solar trackers under varying Direct Beam Fractions (DBF) and total irradiance?

In order to answer the research question, tracker accuracy was binned in both Global Horizontal Irradiances (GHIs) and Direct Beam Fractions (DBFs), with GHI bins of of 200 W/m^2 and DBF bins of 10%. Then the weighted averages of the accuracies were calculated for each single category. Tables 1, 2, and 3 show the results for the three angles measured in the experiment.

One Axis Zomeworks UTR-020 Azimuth Angle

Table 1. *Zomeworks UTR-020 Accuracy % under varying DBF and GHI (Uncertainty 3%)*

DBF%	GHI W/m^2						Weighted Average
	100-300	300-500	500-700	700-900	900-1100	1100-1300	
0-10	68	77	82	N	N	N	70
10-20	64	75	81	85	N	N	75
20-30	51	75	81	81	N	N	76
30-40	44	68	81	84	N	N	73
40-50	45	59	80	85	83	74	75
50-60	46	56	73	85	84	85	77
60-70	27	46	63	83	87	90	74
70-80	33	41	62	79	88	92	70
80-90	N	44	65	85	91	93	83
Weighted Average	67	65	70	83	90	90	75

N: No data in the category.

Table 1 shows that accuracy increases as GHI increases for each of the DBF bins. In addition, it shows that the accuracy decreases as DBF increases for the lower GHI bins. This inverse behavior between accuracy and DBF for the Zomeworks UTR-020 shows a possible explanation of the role played by the aluminum shadow plates that surround the canisters of the tracker. The objective of these plates is to reflect all rays incident on them to heat the working fluid inside the canisters of the tracker. So as DBF increases the diffuse radiation that is received by the reflectors decreases. The increasing amount of DBF doesn't heat the working fluid as the reflected rays do, because the working fluid exists in corners 1 & 2 as shown in Figure 28, which by then the working fluid is more exposed to normal reflected rays than the DBF of the solar radiation. Table 1 also shows that the overall weighted average of the accuracy of the Zomeworks UTR-020 azimuth angle is 75%.

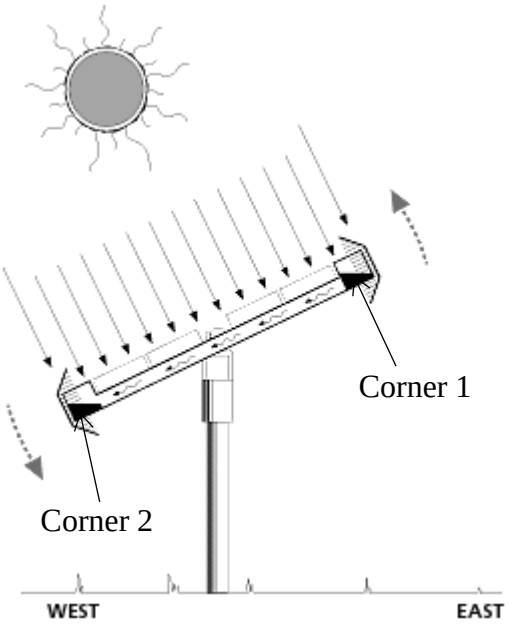

Figure 28. Image of the Zomeworks UTR-020 solar tracker explains the heating of the working fluid (Adapted from Gigawatt, Inc., 2013, image 4).

Two Axis (Wattsun AZ-225) Azimuth and Elevation Angles

Table 2. *Wattsun AZ-225 Azimuth Angle Accuracy % under varying DBF and GHI (Uncertainty 3.5%)*

DBF%	GHI W/m^2						Weighted Average
	100-300	300-500	500-700	700-900	900-1100	1100-1300	
0-10	76	82	83	N	N	N	78
10-20	92	90	88	73	N	N	90
20-30	94	93	92	91	91	N	92
30-40	94	94	94	94	87	N	94
40-50	95	93	93	93	93	86	93
50-60	90	92	93	94	93	91	93
60-70	96	93	94	94	94	94	94
70-80	94	95	93	95	95	95	94
80-90	96	94	92	95	95	95	95
90-100	N	N	96	98	98	N	98
Weighted Average	78	88	92	94	95	94	88

N: No data in the category.

Table 3. *Wattsun AZ-225 Elevation Angle Accuracy % under varying DBF and GHI (Uncertainty 1.4%)*

DBF%	GHI W/m^2						Weighted Average
	100-300	300-500	500-700	700-900	900-1100	1100-1300	
0-10	75	89	95	N	N	N	79
10-20	85	90	95	95	N	N	90
20-30	89	93	95	95	99	N	93
30-40	92	94	96	95	97	N	95
40-50	93	94	96	96	96	95	95
50-60	91	94	95	96	96	96	95
60-70	95	94	94	97	96	96	96
70-80	94	92	93	97	96	96	95
80-90	99	92	93	96	96	97	96
90-100	N	N	94	95	95	95	95
Weighted Average	76	91	94	96	96	96	89

N: No data in the category.

Tables 2 and 3 show the weighted averages of the accuracy increase with increasing GHI. In addition, they show that the weighted averages of the accuracy significantly increased while DBF increased from 10% to 20%, and that the weighted averages of the

accuracy are basically constant and very high for GHI greater than 300 W/m^2 and DBF% greater than 30%. Moreover, they show that the overall weighted averages of the accuracies of both the Wattsun AZ-225 azimuth and elevation angles were 88%, and 89% respectively.

Conclusions from Testing Hypotheses

In this section, findings related to the three research hypotheses are presented. Those research hypotheses were:

H_1. There will be strong positive correlations between tracker accuracy and level of DBF for the Wattsun AZ-225 active altitude and azimuth and the Zomeworks UTR-020 passive azimuth solar trackers.

H_2. The Wattsun AZ-225 active altitude and azimuth tracker will be more accurate than the Zomeworks UTR-020 passive azimuth tracker under strong DBFs and total irradiances.

H_3. There will be weak correlation between the accuracy and the ambient temperature.

The following sub-sections show the results for the three angles measured in the experiment.

First Hypothesis

Table 4. *First Hypothesis Test Results*

Angles Measured	Correlation Coefficients Between Accuracies and DBFs	Observations	Results
Zomeworks Azimuth	**+0.2**	**Weak Positive Correlation**	**Rejected**
Wattsun Azimuth	**+0.6**	**Strong Positive Correlation**	**Accepted**
Wattsun Elevation	**+0.4**	**Moderate Positive Correlation**	**Rejected**
Final Result			**Hypothesis Rejected**

Table 4 shows that the correlation coefficient of the Zomeworks azimuth angle's accuracy and the DBF% is +0.2. It also shows that the correlation coefficient of the Wattsun azimuth angle's accuracy and DBF% is +0.6. In addition, it shows that the correlation coefficient of the Wattsun elevation angle's accuracy and DBF% is +0.4. Because the correlation coefficient of +0.6 is the only coefficient that describes strong correlation, the first Hypothesis is rejected as shown in the bottom of the results column.

Second Hypothesis

In order to test the second hypothesis, two bar charts were plotted. The first one was between the weighted average accuracies and DBF percentages for both the Zomeworks azimuth angle and the Wattsun azimuth angle. The second one was between the weighted average accuracies and GHI for both angles as well. The two charts are shown in Figures 29 & 30.

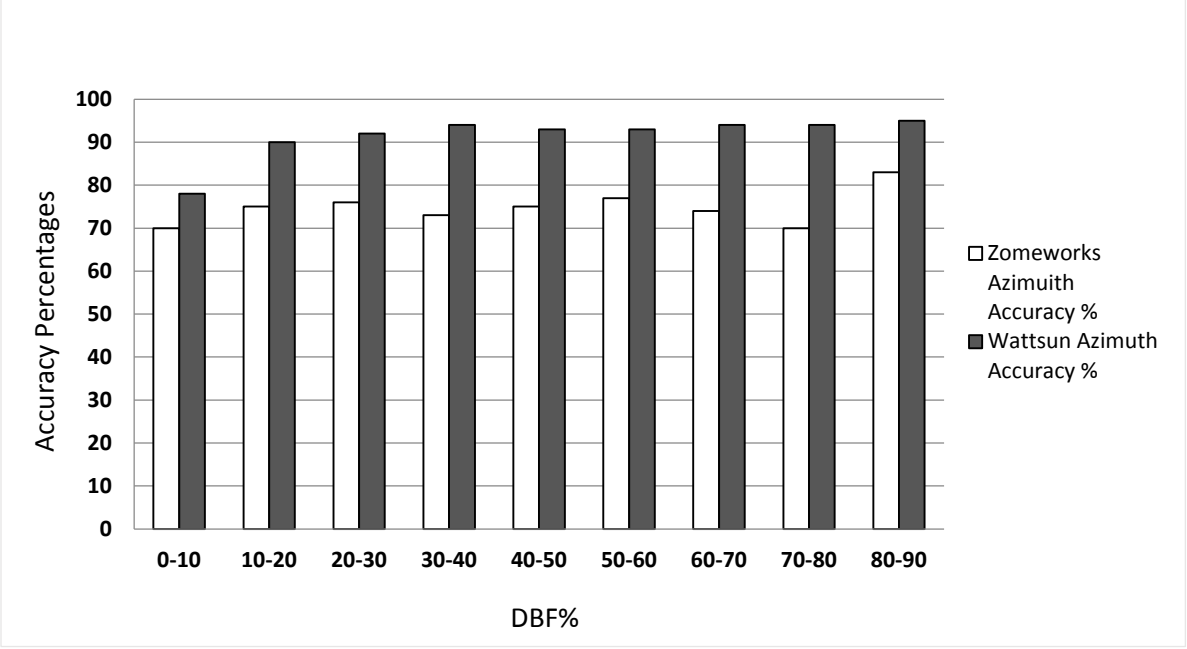

Figure 29. Accuracy percentages and DBF % for Zomeworks and Wattsun azimuth angles.

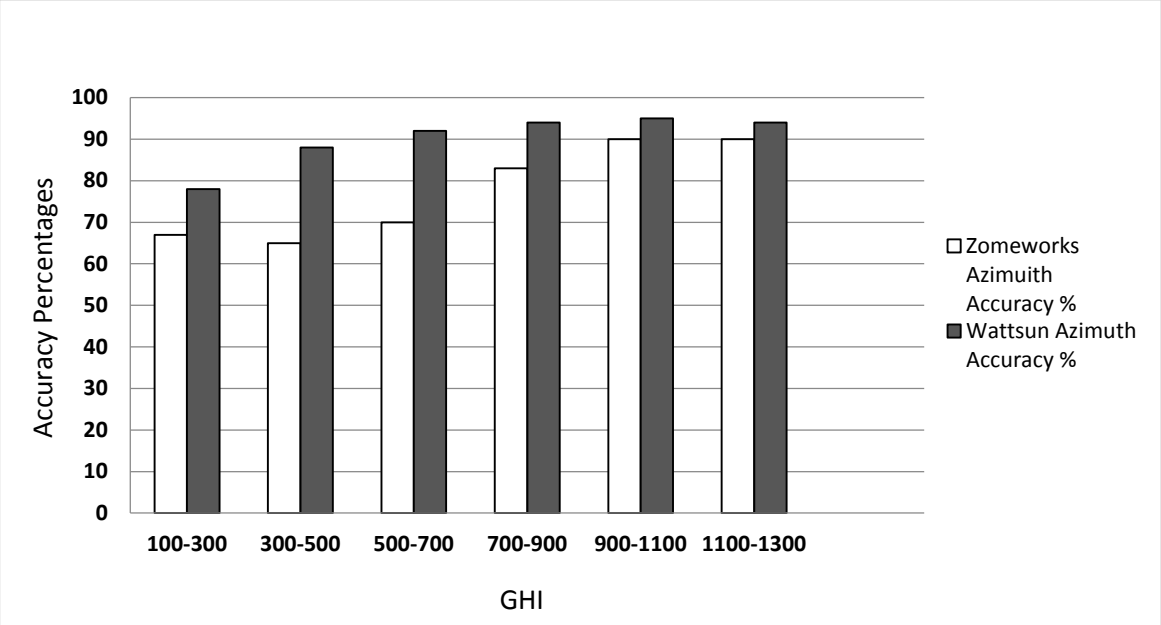

Figure 30. Accuracy percentages and GHI for Zomeworks and Wattsun azimuth angles.

It is shown in Figures 29 and 30 that the Wattsun azimuth angle's accuracy is always higher than that of the Zomeworks azimuth angle under all ranges of both DBF percentages and GHI. Therefore, the second hypothesis is accepted.

Third Hypothesis

Table 5. *Third Hypothesis Test Results*

Angles Measured	Correlation Coefficients Between Accuracies and Ambient Temperature	Observations	Results
Zomeworks Azimuth	**+0.1**	**Very Weak Positive Correlation**	**Accepted**
Wattsun Azimuth	**+0.3**	**Weak Positive Correlation**	**Accepted**
Wattsun Elevation	**+0.2**	**Weak Positive Correlation**	**Accepted**
Final Result			**Hypothesis Accepted**

Table 5 shows that the correlation coefficient of the Zomeworks azimuth angle's accuracy and the ambient temperature is +0.1. It also shows that the correlation coefficient of

the Wattsun azimuth angle's accuracy and ambient temperature is +0.3. In addition, it shows that the correlation coefficient of the Wattsun elevation angle's accuracy and ambient temperature is +0.2. Because all the correlation coefficients are weak or weak correlations, the third hypothesis is accepted.

Daily Behavior of Zomeworks UTR-020 Solar Tracker

Histograms of Zomeworks UTR-020 solar tracker in Appendix A were created from the filtered data that was used in the analysis of this study. As shown in those histograms, the Zomeworks solar tracker leads the sun in the morning and lags the sun in the afternoon. The modes of the histogram of the Zomeworks UTR-020 behaviors from 8:00 am to 4:00 pm illustrate this (Table 6).

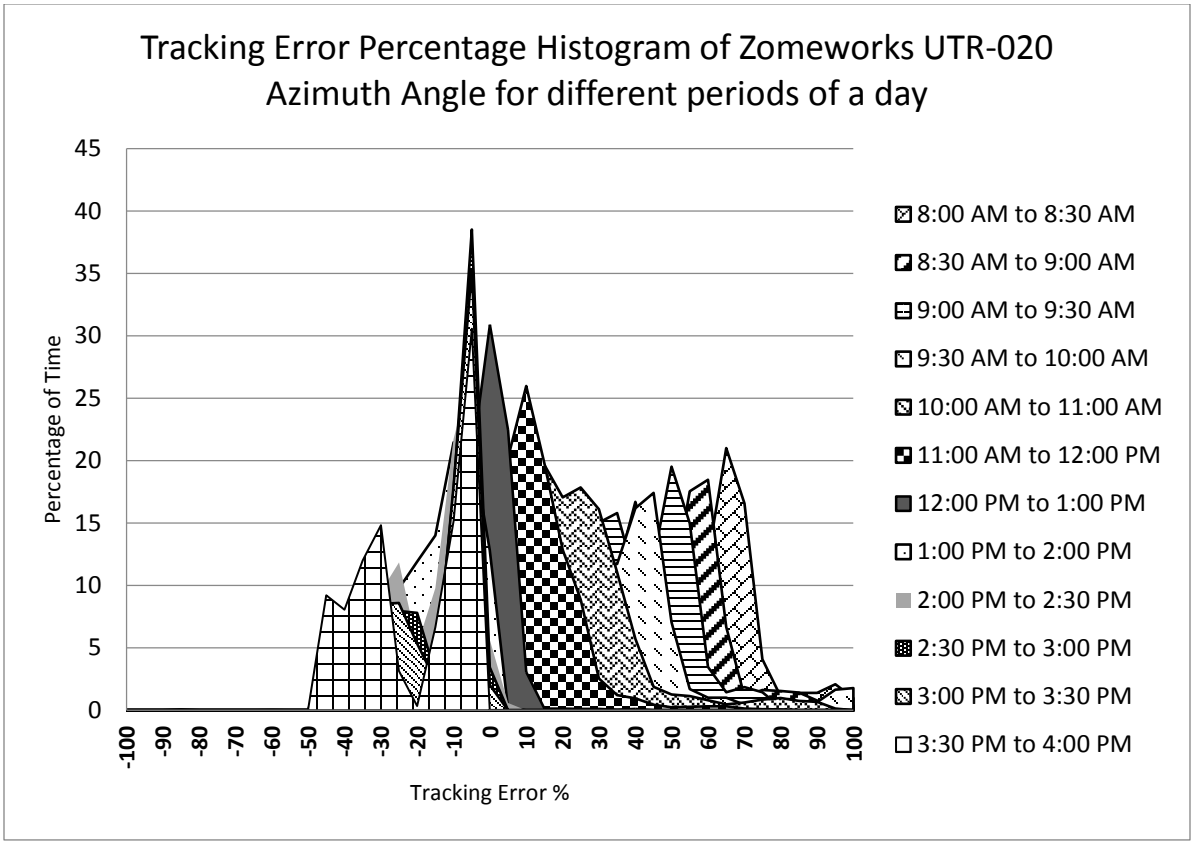

Figure 31. Tracking error percentage histogram of Zomeworks UTR-020 azimuth angle for different periods of a day shows that the tracker leads the sun in the morning and lags the sun in the afternoon through different timed stages.

Table 6. *Modes of Tracking Error Percentages of the Zomeworks UTR-020 Solar Tracker throughout the Day*

Times of the Day	Modes of Tracking Errors %
8:00 am – 8:30 am	+50% & +65%
8:30 am – 9:00 am	+40% & +60%
9:00 am – 9:30 am	+35% & +50%
9:30 am – 10:00 am	+25% & +45%
10:00 am – 11:00 am	+15%
11:00 am – 12:00 pm	+10%
12:00 pm – 1:00 pm	0%
1:00 pm – 2:00 pm	-10%
2:00 pm – 2:30 pm	-5% & -25%
2:30 pm – 3:00 pm	-5%
3:00 pm – 3:30 pm	-5% & -35%
3:30 pm – 4:00 pm	-5% & -30%

Table 6 shows that the Zomeworks solar tracker has large and positive errors in the morning and smaller negative errors in the afternoon. A clear trend is seen from the tracker leading the sun's azimuth in the morning to lagging the sun's azimuth in the afternoon. It is shown in the histograms in Appendix A and from Table 6 that there are three behaviors of the Zomeworks UTR-020 throughout the eight hours of the day and they are almost symmetric around noon time. In the first two hours of the day, the tracker has two different behaviors every half an hour. In the middle four hours of the day, around noon, the tracker had one behavior for every hour. In the last two hours of the day, the tracker has two different behaviors every half an hour as well. It is also clear that a tracking error of -5% was common in the last two hours of the day.

While no definitive explanation of the bimodal distributions was found, the behavior is suggestive. During the morning the tracker has two modes, both of which significantly lag the sun. Two modes are seen as well during the afternoon; however, one of these modes is

near to zero error while the other mode follows the diurnal trend of increased leading. Continued investigation of this behavior is warranted.

Future Research

This research was the first of its kind to fill a gap in the literature by determining the accuracy of solar trackers through direct measurement of their tracking angles. Because this research was done only on two types of solar trackers, further studies could be done on other types of solar trackers. Additional studies could compare the accuracy of different types of solar trackers whether by using the "Angles Method" as this research did/or by using the "Maximum Power Point (MPP) Method" as previous studies have done, or compare them. In addition, this research could be repeated taking into consideration other variables like wind speed and wind direction. This research could be repeated indoors under controlled variables to study the effect of each variable on the accuracy of solar trackers. Moreover, this research could be repeated in other locations.

Another important parameter could be the focus of future research, which would be to examine the economic values of different solar trackers. Differences in solar trackers relative accuracy could affect the market.

Several modifications could be tested in the design of the Zomeworks UTR-020 solar tracker as well. The cross section of the canisters that act as actuators could be changed to reach better heating of the working fluid. Different materials of these canisters could be developed in order to reach higher absorptivity and lower reflectivity to ensure better heating of the working fluid. Different shapes, materials, or coatings of the aluminum shadow plates could be implemented to enhance the reflectivity. New materials could be tested for the working fluids for example; nano-materials perform in a totally different way than

macroscopic materials. Further research could be done to investigate for different Nano-materials that could be used as the working fluid of the Zomeworks actuators.

Final Remarks

This research was undertaken to measure the solar tracking angles of the Zomeworks UTR-020 and the Wattsun AZ-225 solar trackers in order to determine their tracking accuracy. The measured angles were the surface azimuth angles of both the Zomeworks and the Wattsun solar trackers, and the solar elevation angle, which is the complementary angle of the surface elevation angle and the inclination angle of the Wattsun solar tracker when the incidence angle equals to zero (as explained in Chapter 2, Solar Tracking Geometry section). For complete accuracy, the surface azimuth angles of the Zomeworks and the Wattsun solar trackers should be equal to the solar azimuth angle when the incidence angle equals zero as well (as explained in Chapter 2, Solar Tracking Geometry section).

This method of determining the accuracy of solar trackers by measuring angles was called “Angles Method to determine the accuracy of solar trackers” (as explained in Chapter 3, Data Analysis Procedures section). In contrast to many other studies showing the advantages of using tracking systems, this research didn’t measure the power generated by the solar panel systems that incorporated the Zomeworks UTR-020 and Wattsun AZ-225 solar trackers. Instead, it sought to closely examine the degree to which these tracking systems were able to achieve optimal solar angles (optimal accuracy) over the course of a day and under different operating conditions.

REFERENCES

Baltas, P., Tortoreli, M., & Russell, P. (1986). Evaluation of power output for fixed and step tracking photovoltaic arrays. *Solar Energy, 37* (2), 147-163. Retrieved from http://www.sciencedirect.com/science/article/pii/0038092X86900721

Braun, J. E., & Mitchell, J.C. (1983). Solar geometry for fixed and tracking surfaces. *Solar Energy*, *31*(5), 439-444. Retrieved from http://www.sciencedirect.com/science/article/pii/0038092X83900464

Catarius, A., & Christiner, M. (2010). *Azimuth-altitude dual axis solar tracker* (Unpublished honor's thesis). Worcester Polytechnic Institute, Worcester, MA. Retrieved from http://www.wpi.edu/Pubs/E-project/Available/E-project-121710-140419/unrestricted/Dual_Axis_Tracker_Final_Report.pdf

Clifford, M. J., & Eastwood, D. (2004). Design of a novel passive solar tracker. *Solar Energy*, *77*(3), 269-280. Retrieved from http://www.sciencedirect.com/science/article/pii/S0038092X04001483

Gigawatt, Inc. (2013). Zomeworks Track Rack UTR020 Universal Solar Tracker [image]. Retrieved from http://www.gogreensolar.com/products/zomeworks-track-rack-utr020-universal-solar-tracker-20-sq-ft

Helwa, N. H., Bahgat, A. G., El Shafee, A. R., & El Shenawy, E. T. (2000). Computation of the solar energy captured by different solar tracking systems. *Energy Source, 22*(1), 35-44. Retrieved from http://www.tandfonline.com/doi/abs/10.1080/00908310050014199

Huang, Y. J., Kuo, T. C., Chen, C. Y., Chang, C. H., Wu, P. C., & Wu, T. H. (2009). The Design and Implementation of a Solar Tracking Generating Power System. *Engineering Letters, 17* (4), 1-5. Retrieved from http://www.engineeringletters.com/issues_v17/issue_4/EL_17_4_06.pdf

Iqbal, M. (1983). *An introduction to solar radiation*. Toronto: Academic Press. Retrieved from http://www.iac.ethz.ch/edu/courses/bachelor/vertiefung/climate_systems/notizen/Solar-Radiation-Radiative-Transfer.pdf

Mazria, E. (1979). *The passive solar energy book.* Emmaus. PA: Rodale Press.

McDonald, M. (2010). U.S. Patent Application No. 0018518 A1. Washington, DC: U.S. Patent and Trademark Office. Retrieved from http://patentscope.wipo.int/search/en/WO2010011529

Michalsky, J. (1988). *The Astronomical Almanac*'s algorithm for approximate solar position (1950–2050). *Solar Energy, 40*(3), 227-235. Retrieved from http://www.sciencedirect.com/science/article/pii/0038092X8890045X

Mousazadeh, H., Keyhani, A., Javadi, A., Mobli, H., Abrinia, K., & Sharifi, A. (2009). A review of principle and sun-tracking methods for maximizing solar systems output. *Renewable and Sustainable Energy Reviews, 13*(8), 1800-1818. Retrieved from http://www.sciencedirect.com/science/article/pii/S1364032109000318

Oh, S. J., Hyun, J. H., Lee, Y. J., Chen, K., Choon, N. K., Lee, Y. S., & Chun, W. (2009, September). *A study on the development of high accuracy solar tracking systems*. Paper presented at 8th International Conference on Sustainable Energy Technologies, Aachen, Germany. Retrieved from http://www.slideshare.net/iskandaruz/a-study-on-the-development-of-high-accuracy-solar-tracking-systems

Patil, J. V., Nayak, J. K., & Sundersingh, V. P. (1997). Design, fabrication and preliminary testing of a two-axis solar tracking system. *RERIC International Energy Journal*, *19*(1), 15-23. Retrieved from http://www.thaiscience.info/journals/Article/Design,%20fabrication%20and%20preliminary%20testing%20of%20a%20two-axes%20solar%20tracking%20system.pdf

Peterson, T., Rice, J., & Vane, J. (2005). *Solar tracker.* Unpublished manuscript, Cornell University, Ithaca, NY. Retrieved from https://instruct1.cit.cornell.edu/Courses/ee476/FinalProjects/s2005/tp62/website/solar tracker.pdf

Poulek, V., & Libra, M. (n.d.). *New bifacial solar trackers and tracking concentrators.* CiteSeerX Database. Retrieved from http://www.google.com/url?sa=t&rct=j&q=&esrc=s&frm=1&source=web&cd=1&ved=0CC8QFjAA&url=http%3A%2F%2Fciteseerx.ist.psu.edu%2Fviewdoc%2Fdownload%3Fdoi%3D10.1.1.194.9288%26rep%3Drep1%26type%3Dpdf&ei=EPj3UZveK4bO8wTL0IDACg&usg=AFQjCNERRLZOqPIN1lHrSy4F6-jwcfdd9w&sig2=hG0HDxYUvvPKB1ZXsEH9iQ&bvm=bv.49967636,d.eWU

Reda, I., & Andreas, A. (2003). Solar position algorithm for solar radiation applications. *Solar Energy, 76*(5), 577-589. Retrieved from http://www.mikrocontroller.net/attachment/157160/NREL_SPA.pdf

Reno, M., Hansen, C., & Stein, J. (2012). *Global horizontal irradiance clear sky models: Implementation and* analysis (SAND Report 2012-2389). Albequerque, NM: Sandia National Laboratories. Retrieved from http://prod.sandia.gov/techlib/access-control.cgi/2012/122389.pdf

Robinson, J., & Raichle, B. (2012, May). *Performance comparison of fixed, 1-, and 2- axis tracking systems for small photovoltaic systems with measured direct beam fraction*. Paper presented at the 2012 World Renewable Energy Forum, Denver, CO. Retrieved from http://tec.appstate.edu/sites/tec.appstate.edu/files/pv%20tracking%20system%20performance%20and%20direct%20beam%20robinson%20raichle.pdf

Rockwell Automation (2009). *Solar tracking application* [White Paper]. Marion, NC: Rockwell Automation. Retrieved from http://literature.rockwellautomation.com/idc/groups/literature/documents/wp/oem-wp009_-en-p.pdf

Rodriguez, D. (2011). *Mechatronics application of solar tracking* (Unpublished master's thesis). Purdue University, Purdue, IN. Retrieved from http://docs.lib.purdue.edu/techdirproj/34

Sefa, I., Demirtas, M., & Colak, I. (2009). Application of one-axis sun tracking system. *Energy Conversion and Management, 50,* 2709-2718. Retrieved from http://www.sciencedirect.com/science/article/pii/S0196890409002349

Stafford, B., Davis, M., Chambers, J., Martinez, M., & Sanchez, D. (2009, June). *Tracker accuracy:Field experience, analysis, and correlations with meteorological conditions.* Paper presented at the 34th Photovoltaic Specialists IEEE Conference (PVSC). Retrieved from http://ieeexplore.ieee.org/xpl/login.jsp?tp=&arnumber=5411362&url=http%3A%2F%2Fieeexplore.ieee.org%2Fxpls%2Fabs_all.jsp%3Farnumber%3D5411362

Stine, W., & Harrigan, R. (1985). *Solar energy fundamentals and design.* New York: John Wiley.

APPENDICES

Appendix A: Zomeworks Daily Behavior

From 8:00 AM to 4:00 PM

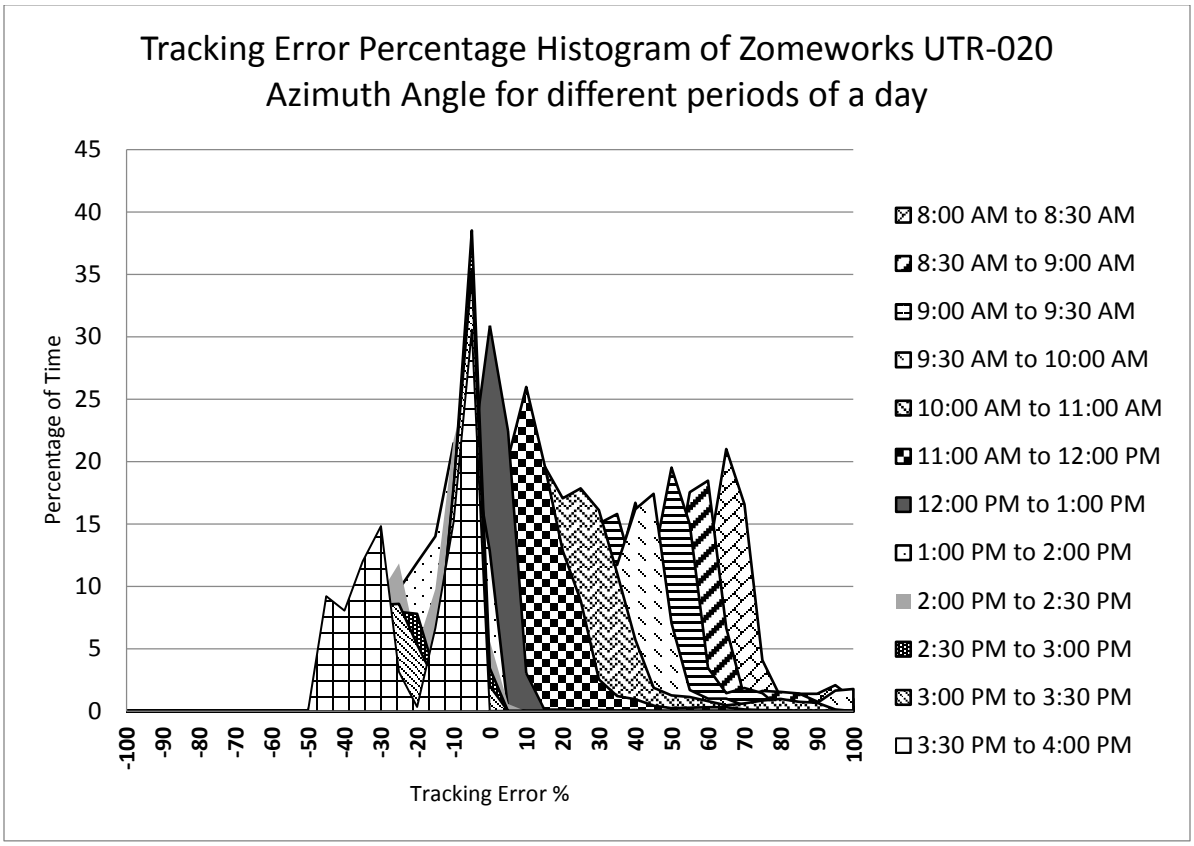

From 8:00 AM to 8:30 AM

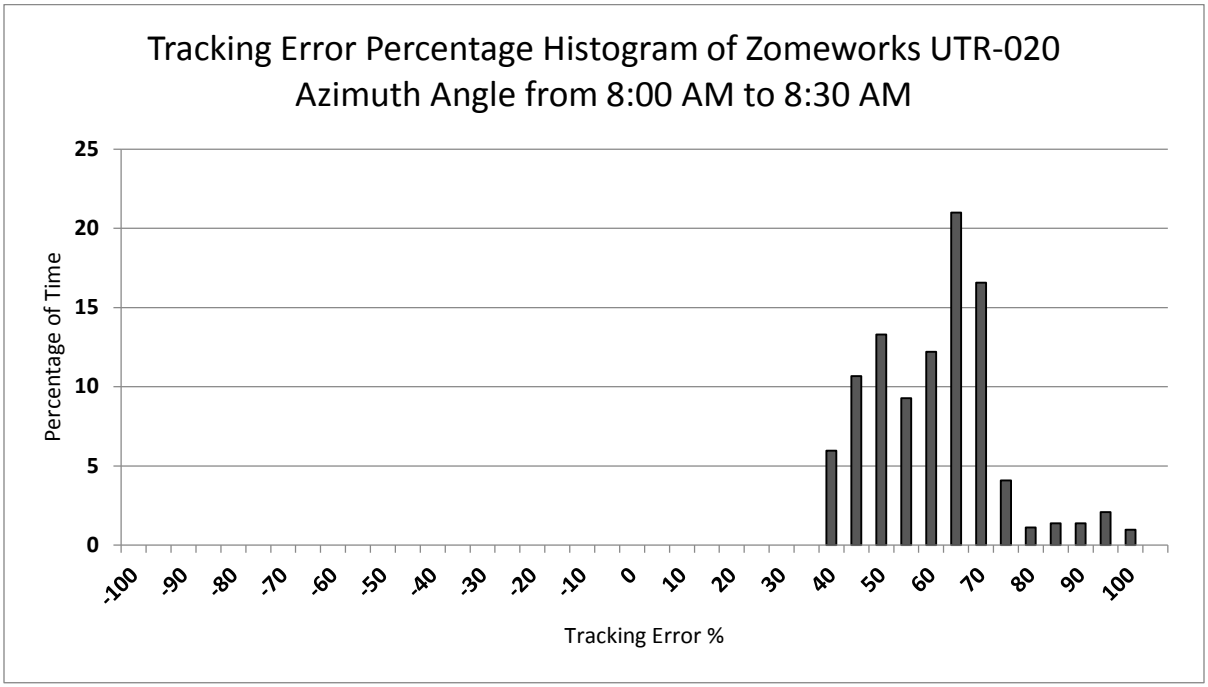

From 8:30 AM to 9:00 AM

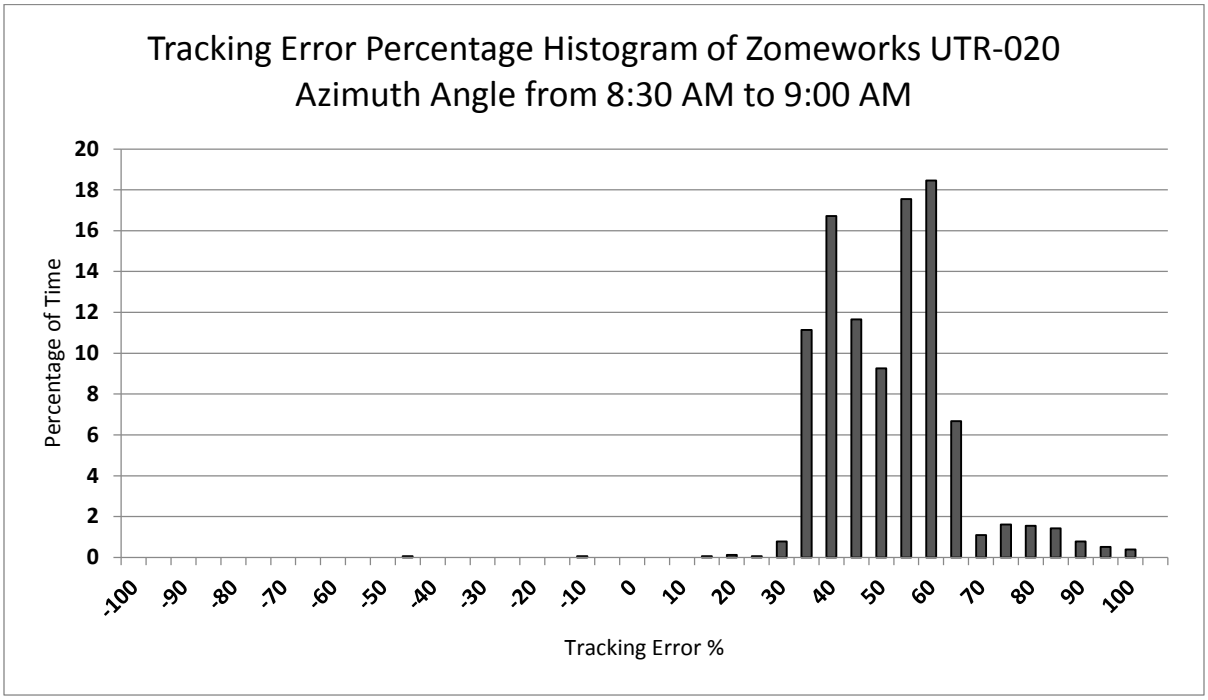

From 9:00 AM to 9:30 AM

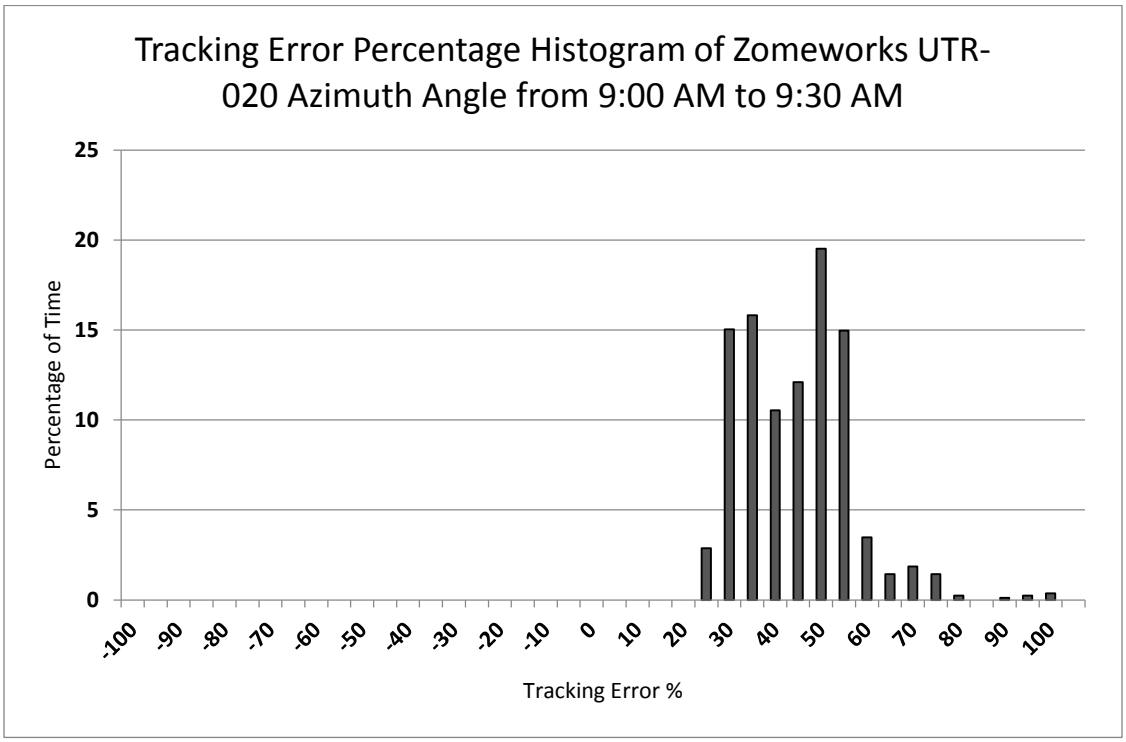

From 9:30 AM to 10:00 AM

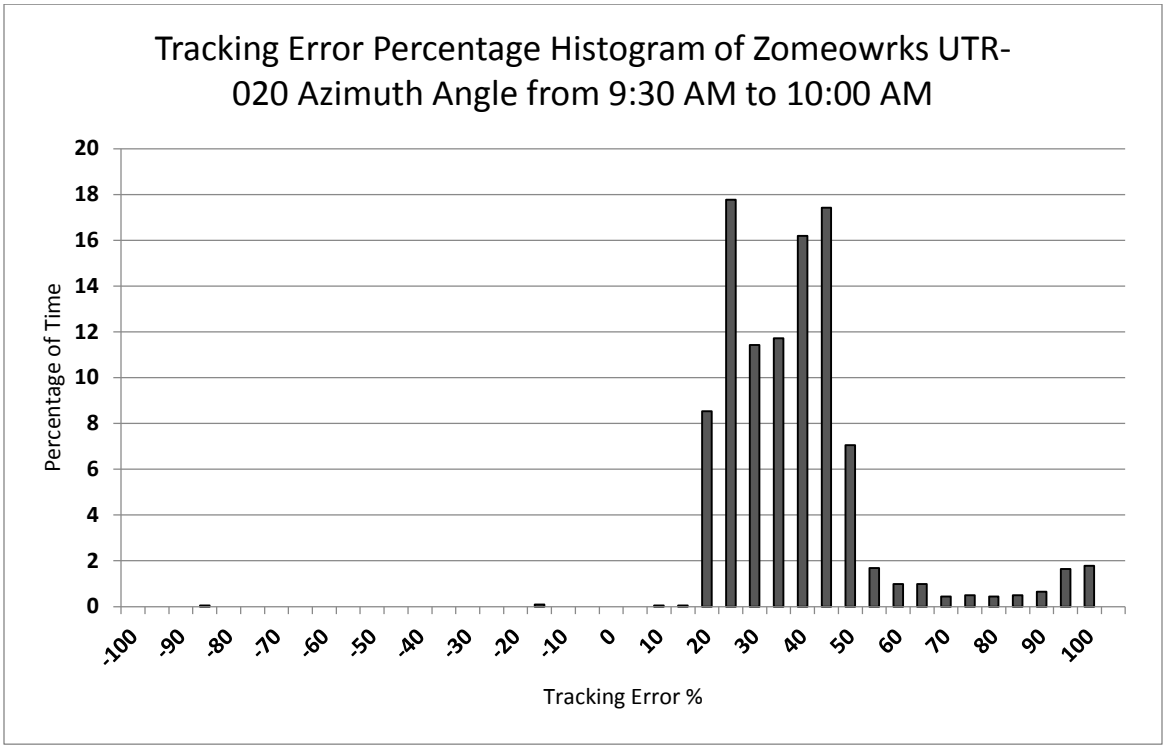

From 10:00 AM to 11:00 AM

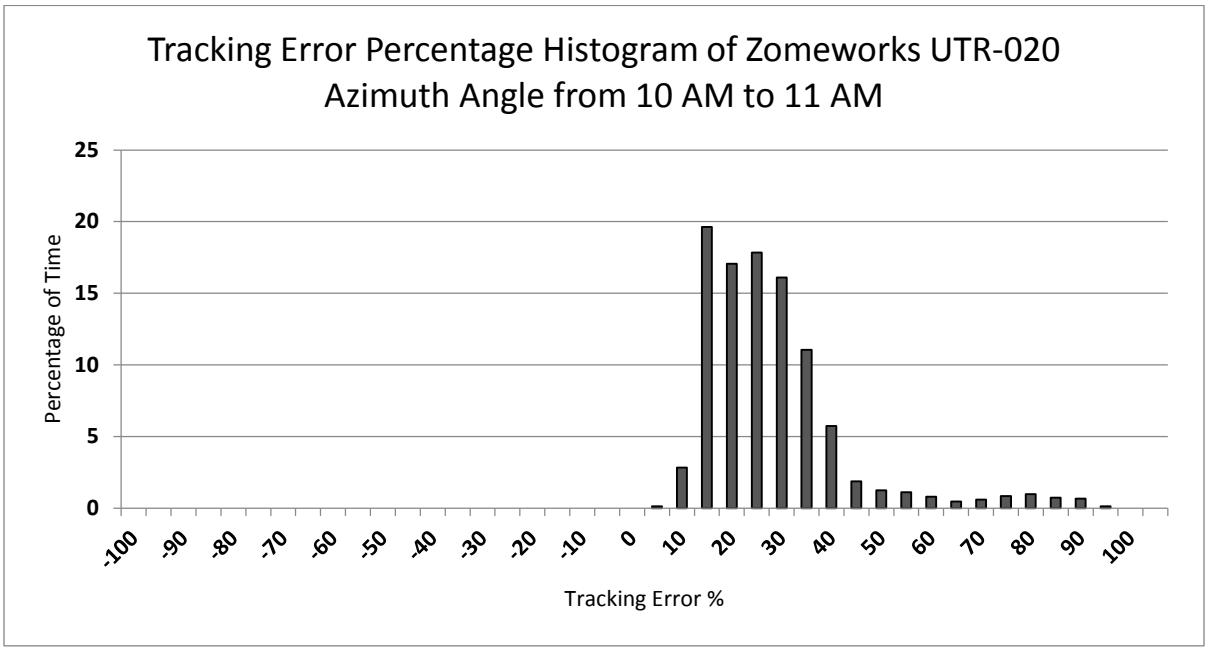

From 11:00 AM to 12:00 PM

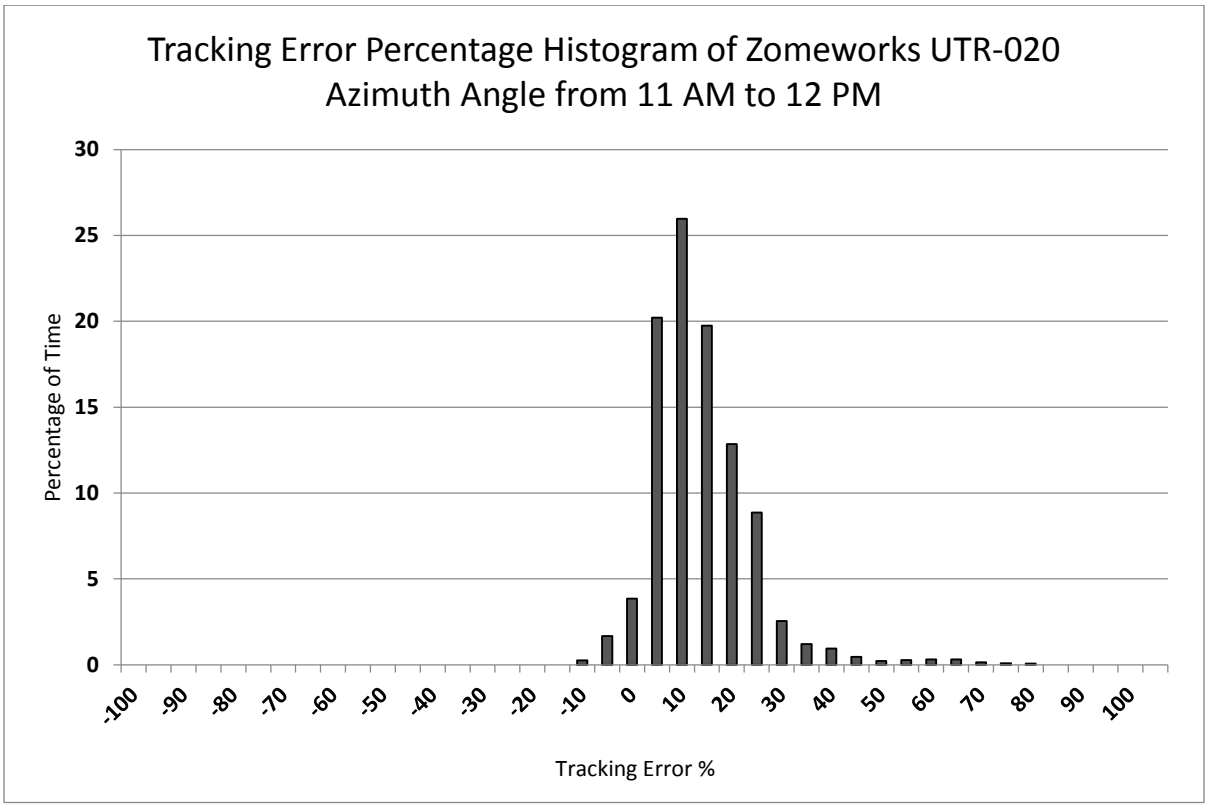

From 12:00 PM to 1:00 PM

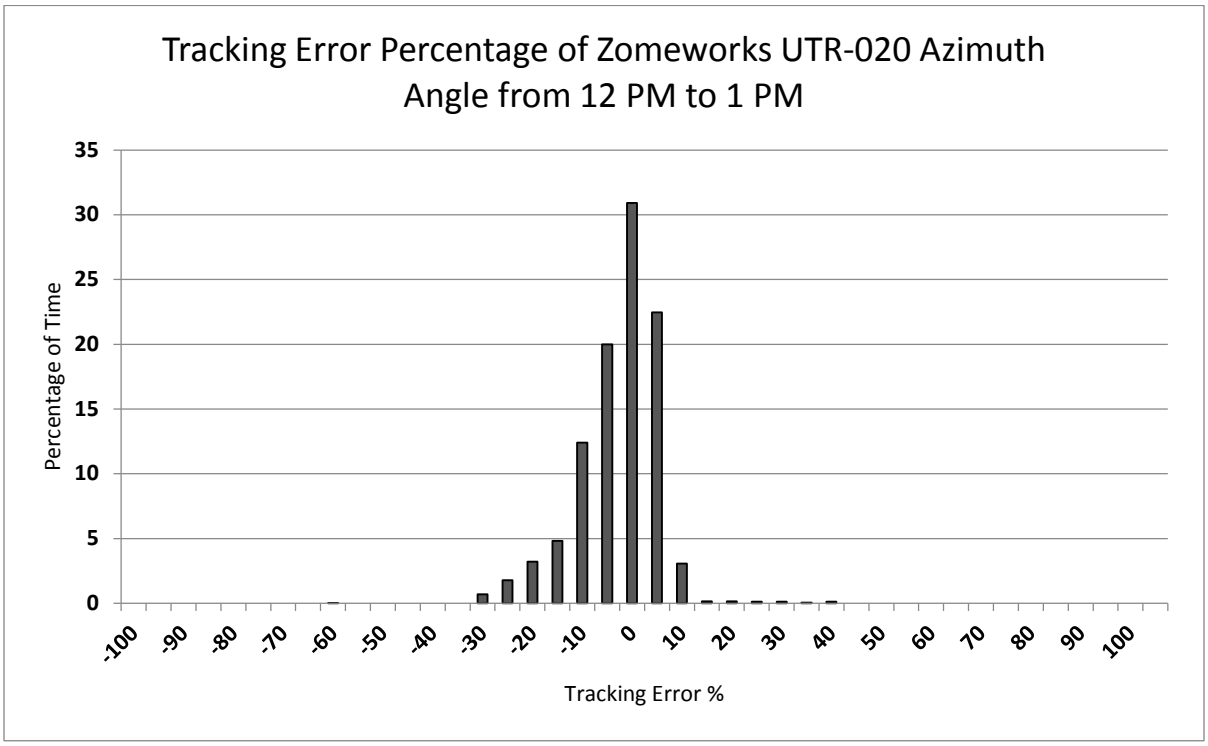

From 1:00 PM to 2:00 PM

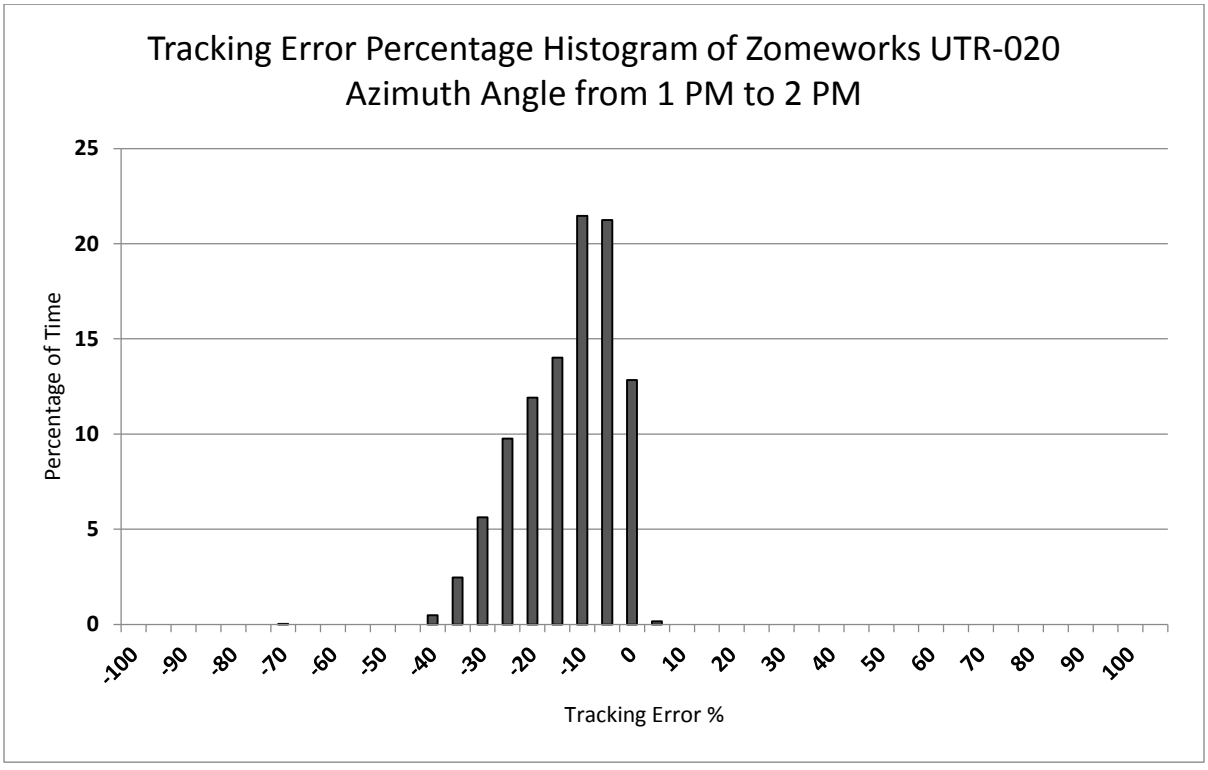

From 2:00 PM to 2:30 PM

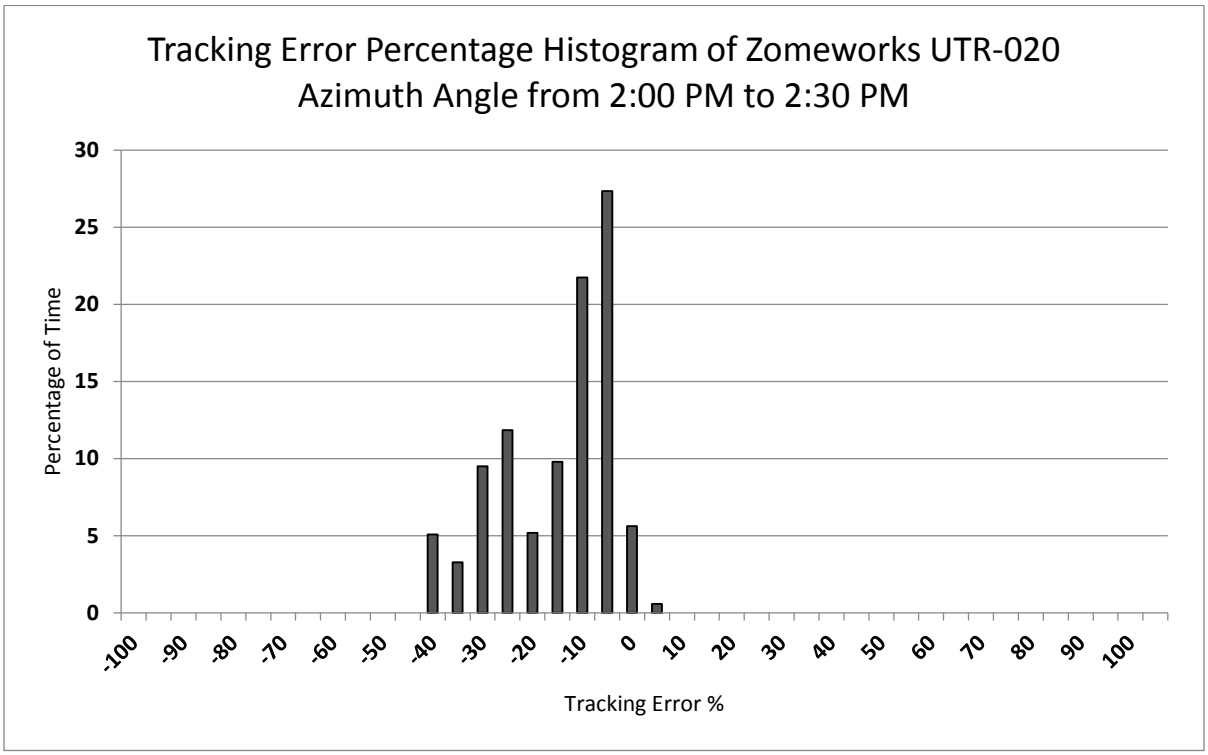

From 2:30 PM to 3:00 PM

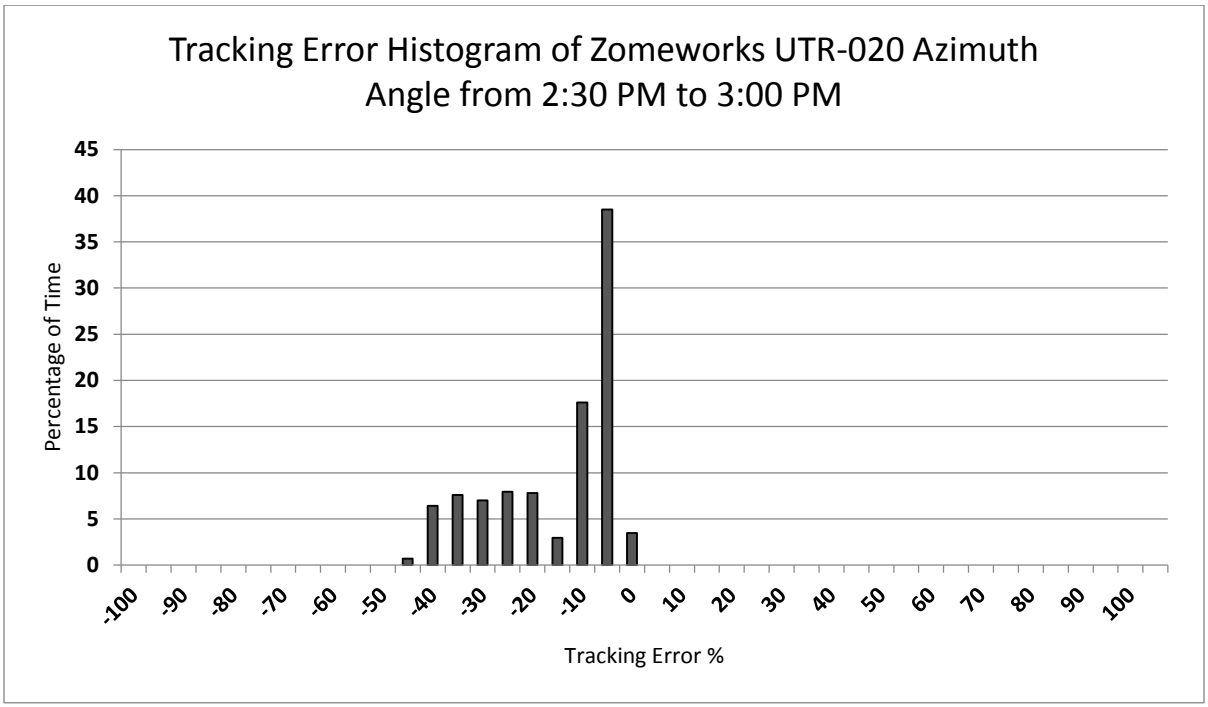

From 3:00 PM to 3:30 PM

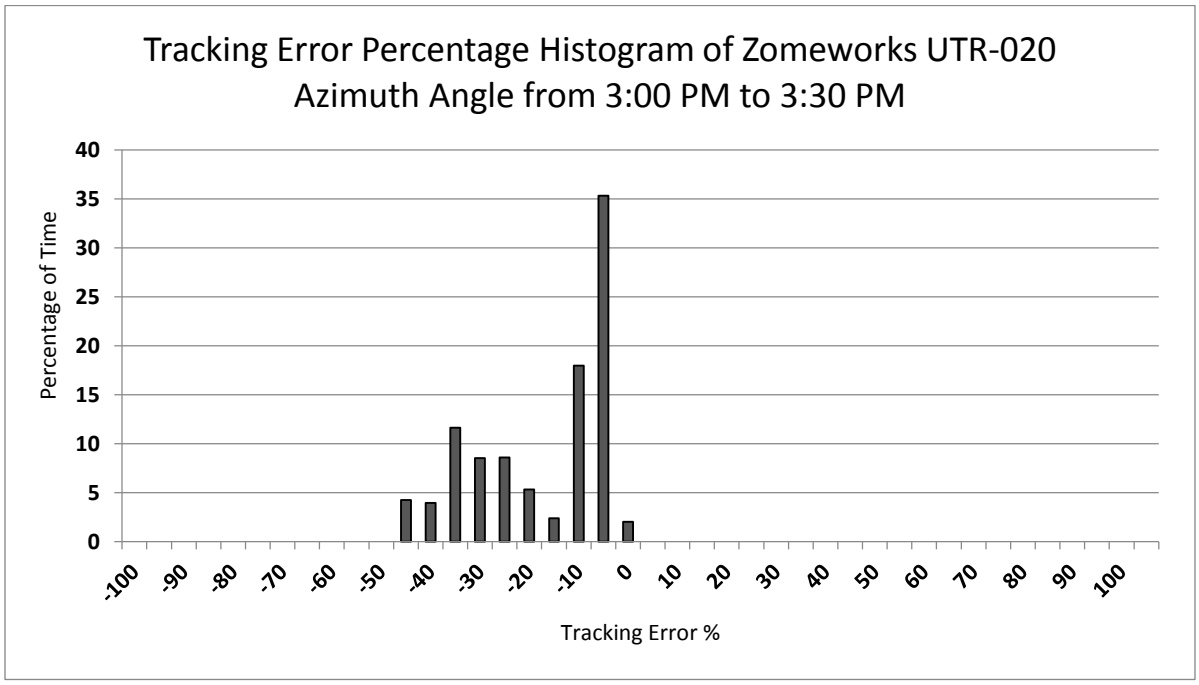

From 3:30 PM to 4:00 PM

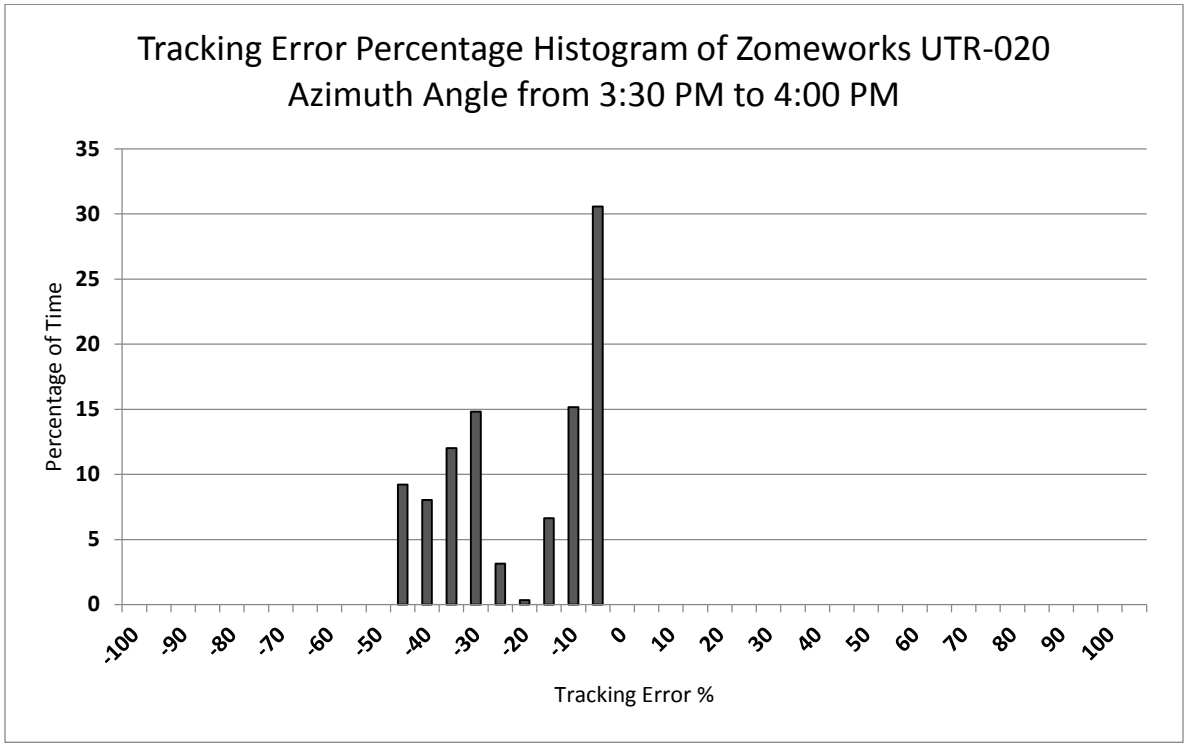

Appendix B: Solar Trackers Used in the Experiment

Zomeworks UTR Brochure

ZOMEWORKS CORPORATION

Passive Energy Products

Environmentally and Financially Sustainable; do not rely on Hydrocarbons or Tax Credits

UNIVERSAL TRACK RACK™

PASSIVE SOLAR TRACKER FOR PHOTOVOLTAIC MODULES

Incorporating over three decades of tracker design and fabrication experience, the UTRF Series Tracker is our most popular design for large arrays. It features sturdy welded-steel construction, pre-assembled bolt-together components, sealed-axle ball bearings, heavy-duty shock absorbers, and early morning wake-up fin to catch the first sunlight of the day. Our UTRK-040 and our UTR-020 are perfect for small PV systems and pumps.

ABC EXTREME MAKEOVER "YAZZIE FAMILY" HOME FEATURING ZOMEWORKS UNIVERSAL TRACK RACK™ MODEL UTRF-168 "THE EARLY BIRD'S VIEW" INSTALLED BY MARK SNYDER ELECTRIC

UNIVERSAL TRACK RACK™ MODEL UTRF-120 PUMPING WATER FOR LIVESTOCK NEAR LORDSBURG, NM

UNIVERSAL TRACK RACK™ MODEL UTRK-040 PHOTO PROVIDED BY TOTAL LIGHT AND POWER

Simplicity and Elegance

Gravity turns the tracker, using the heat from the sun to move liquid from one side to the other side, to reliably track the sun's path from east to west. No motors, no gears and no controls to fail.

Universal

Six standard UTR and UTR-F Track Racks™ fit all common photovoltaic modules. Review our website for a complete list of products, specifications and prices.

Easy to Transport

The Universal Track Rack™ is "knocked down" and packed in one to five packages. (depending on the size of the rack)

SOLD THROUGH A WORLDWIDE NETWORK OF DEALERS

FOR MORE INFORMATION ON DEALERS, SIZING, PRICING, AND OTHER PRODUCTS
VISIT OUR WEBSITE
WWW.ZOMEWORKS.COM

UNIVERSAL TRACK RACK™ PASSIVE SOLAR

TRACK RECORD

Zomeworks has been a leader in passive solar energy products since 1969. The Universal F-Series Track Rack™ is the latest in a long line of Zomeworks photovoltaic mounting structures. Since 1980, more than 17,000 Zomeworks tracking systems have been installed in different climates, on nearly every continent on earth. As dependable as gravity and as reliable as the heat of the sun, more than 99% of our trackers are still in operation today.

COST EFFECTIVE

Zomeworks Track Racks™ increase electrical output of photovoltaic modules by 25% or more compared to modules on fixed mounts. A 12-module tracking system delivers the same electric output as 15 modules mounted on fixed racks – a savings of three modules.

Track Racks™ are highly cost-effective components for domestic and industrial photovoltaic power systems, water pumping systems, cathodic protection systems, and utility applications.

SIX SIZES FIT ALL

Zomeworks UTR-020, UTRK-040 and UTRF Series combine the ingenuity, dependability, and practicality that represent Zomeworks' products with a universality of application that reduces the cost and simplifies the installation of solar systems.

Our six standard sizes hold 2-16 modules. All Universal Track Racks™ will accommodate most PV modules on the market.

These trackers come packaged as a kit with all hardware and instructions for quick assembly. Because just six basic sizes cover the entire range of needs, Zomeworks and its distributors are able to eliminate most special order delays.

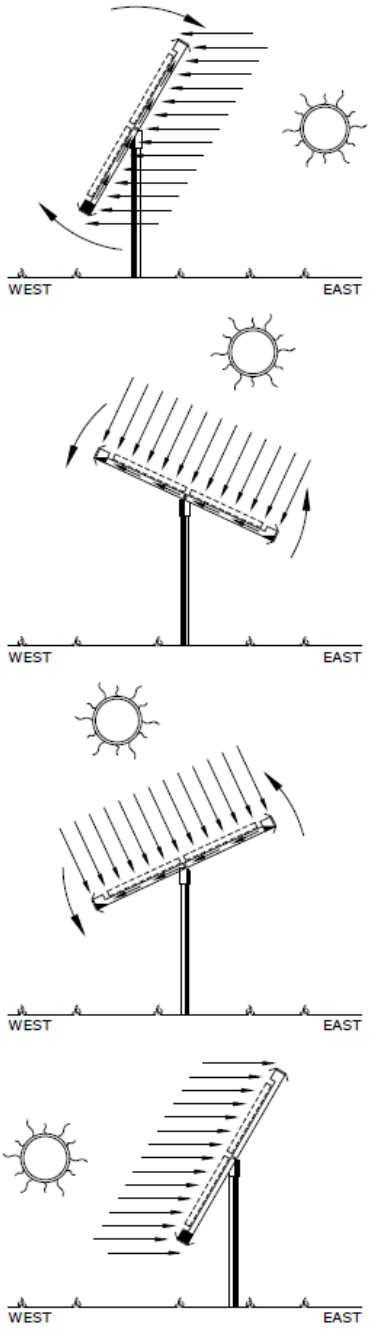

How the Universal Track Rack™ Follows the Sun...

The UTR begins the day facing west. As the sun rises in the east, it heats the unshaded west-side canister, forcing liquid into the shaded east-side canister. As liquid moves through a copper tube to the east-side canister, the tracker rotates so that it faces east.

The heating of the liquid is controlled by the aluminum shadow plates. When one canister is exposed to the sun more than the other, its vapor pressure increases, forcing liquid to the cooler, shaded side. The shifting weight of the liquid causes the rack to rotate until the canisters are equally shaded.

As the sun moves, the rack follows (at approximately 15° per hour), continually seeking equilibrium as liquid moves from one side of the tracker to the other.

The rack completes its daily cycle facing west. It remains in this position overnight until it is awakened by the rising sun the following morning.

ZOMEWORKS CORPORATION
ESTABLISHED 1969
Post Office Box 25805 (1011 Sawmill Rd. NW) Albuquerque, New Mexico 87125
Website: www.zomeworks.com email: zomework@zomeworks.com
[800] 279-6342 [505] 242-5354 phone [505] 243-5187 fax

Wattsun Brochure

About Array Technologies

Array Technologies, Inc., is the leading manufacturer of active solar tracking systems. Homeowners, small businesses, and corporations worldwide use our tracker drives, electronic tracking controls, and consult with our solar electric experts. Our products and services are used for the following purposes:

Wattsun™ AZ-225 Dual Axis Tracker Capacity of over 3 kW of PV's.

- Utility scale PV systems
- Grid-tie residential
- Grid-tie commercial
- Off-grid remote homes
- PV solar water pumping systems
- Exposure testing laboratories
- Telecommunications systems
- Museum and art exhibits
- Small-scale concentrator PV systems
- Indoor day lighting systems

Wattsun™ AZ-225 Single Axis Tracker. 2.4 kW Residential installation.

For more information about Wattsun™ Solar Trackers contact:

Dealer information here.

Array Technologies, Inc.
3312 Stanford NE
Albuquerque, NM 87107
Tel: 505.881.7567 / Fax: 505.881.7572
Email: sales@wattsun.com
URL: www.wattsun.com

WATTSUN™
SOLAR TRACKERS

WATTSUN™
SOLAR TRACKERS

For efficient, renewable energy systems.

Array Technologies, Inc.

Visit us at: www.wattsun.com

Intelligent Solar Tracking Systems

MAXIMUM POWER PRODUCTION.
Sensible choice.

With a Wattsun™ Solar Tracker your PV system finally achieves its maximum power production. That's because *all day long* Wattsun Trackers automatically move your PV array to precisely aim at the sun. Your Wattsun Tracker can produce up to 40% more power annually than with a fixed array mount, depending on where you live. That makes Wattsun Trackers the most sensible and economical choice.

Wattsun™ AZ-225 Solar Trackers

INDEPENDENT POWER.
Renewable and efficient.

Whether powering your home or pumping water, Wattsun Trackers provide power where and when you need it. Wattsun Trackers even harvest the sun's energy when fixed arrays can't: early in the morning when your batteries are at their lowest, as well as, late in the afternoon, when electric demand might be at its peak.

QUALITY DESIGN.
High tech products.

For very large commercial and utility scale PV systems, **Array Technologies** offers single axis *Horizontal-Axis Trackers*. and *Fixed Tilt Azimuth Trackers*. They are well suited for high-density, large scale utility PV projects.

For medium-to-large residential and commercial PV systems, **Array Technologies** manufactures *Azimuth Trackers*. The azimuth tracker gear drive rotates the PV array on the pole mount so the bottom edge of the array always remains parallel to the ground. The result: exceptional stability in the wind. The dual axis option enables automatic up-and-down movement. Dual axis azimuth trackers completely capture all the power the sun delivers.

Wattsun™ 2.4 kW AZ-225 in Goshen, Indiana

WATTSUN™
SOLAR TRACKERS

SUPERIOR PERFORMANCE.
Durable construction.

Environmentally-friendly, Wattsun active trackers are guided by a patented, optical sun-sensing device, which dramatically outperforms passive tracking systems. Solid state electronic design and positive drive mechanisms insure consistent operation in extreme temperatures and windy conditions.

Wattsun™ AZ-225, Reno, Nevada

Each tracker frame is precisely engineered for strength and rigidity, fabricated from corrosion-resistant structural aluminum and easily assembled onsite.

BIG REWARD.
Little effort.

Manufactured from the finest quality materials, Wattsun™ Trackers are easy to install, easy to operate and inexpensive to maintain. For more information, visit us on the web at wattsun.com or talk to your local solar electric dealer.

Minitrack II Solar Tracker (Michalsky's Celestial Algorithm Based) Used to get the Actual Sun Angles

MINITRAK II™

SOLAR TRACKER

The MiniTrak II™ solar tracker is the most cost effective autonomous two-axis radiometer tracking platform on the market bar none. With mounting accommodation for up 10 normal incidence pyrheliometers and/or multiple normal incidence mounted pyranometers and one global horizontal diffuse (shaded) pyranometer, the MiniTrak II™ is ideally suited to meet virtually any solar monitoring application requirement.

The MiniTrak II™ was developed by Precision Solar Technologies Corp. (PST) in cooperation with engineers at Sandia National Laboratories, to provide an accurate, durable and cost effective autonomous solar tracking solution for the solar renewable and climate monitoring research communities. Costing thousands less than competing radiometer tracker models, the MiniTrak II™ offers the greatest DNI pyrheliometer mounting capacity in the industry; up to 10 Hukseflux DR01 model pyrheliometers can be mounted 'standard'. In addition to pyrheliometer mounting, the MiniTrak II™ can also accommodate the mounting of any Hukseflux model pyranometer in either the global horizontal or POA (plane of array) mode. When properly equipped the MiniTrak II™ is suitable for:

- **Normal incidence direct solar irradiance measurement**
- **Global solar irradiance measurement (horizontal)**
- **Global diffuse irradiance measurement (horizontal)**
- **Global solar irradiance measurement (POA)**
- **Global diffuse irradiance measurement (POA)**

FEATURES

- **Precision reflective optical alignment pointer**
- **Integrated 20 Watt PV rechargeable battery system**
- **Embedded system controller (no host PC required)**
- **Shading options for horizontal and/or POA mounted pyranometers (diffuse)**

"Due to its extraordinary value, application flexibility and reliability, the MiniTrak II™ has been sold to universities, government laboratories and industry Worldwide."

APPLICATIONS

- **Solar renewable resource assessment**
- **Climate research**
- **Material testing /weathering studies**

Note: Above applications are inclusive of, but not limited to the MiniTrak II's entire application range.

MINITRAK II™ SPECIFICATIONS

Tracking mode:	via celestial calculation algorithm
Positioning accuracy:	±0.25° (4 mrad) min.
Velocity:	1.8°/ sec
Acceleration:	3.9°/ sec²
Torque:	15 Nm / 11 ft-lbs (azimuth) 136 Nm / 100 ft-lbs (zenith)
Payload (balanced):	32kg (70 lbs)
Altitude:	any altitude
Rotation limit (azimuth):	270° degrees (standard)
Elevation limit (zenith):	90° degrees (standard)
Operating temperature:	-40° to +80° C
Weight (uncrated):	34 kg / 75 lbs (tracking platform) 34 kg / 75 lbs (controller / battery)
Clock accuracy:	± 15 sec / year (after calibration) onboard battery backup GPS clock synch optional available
PC connectivity:	RS232C Fiber optic COMM available
Interface software:	NI LabVIEW
PV charging system:	20 Watt PV panel (standard) 24 VDC / 35 amp hour battery
Mounting:	pole mount, 3" inch diameter
Ground clearance:	18" inches min., or >
Radius clearance:	36" inches min.

P.O. Box 850
Manorville, NY 11949
T: 631-251-6963
F: 631-657-0364
E: info@HuksefluxUSA.com
W: www.HuksefluxUSA.com

HuksefluxUSA™
Thermal Sensors

MINITRAK II™ SOLAR TRACKER

▲ *Figure 1: PST Prospector™ system with MiniTrak II™ and fully integrated turnkey weather monitoring station*

▲ *Figure 2: SolarTrak® electronics controller and battery box enclosures*

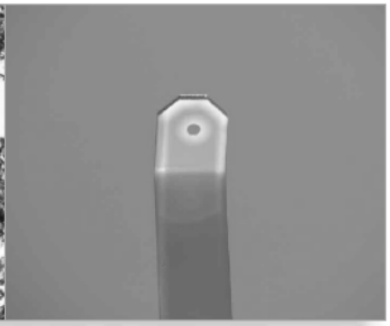

▲ *Figure 3: Precision reflective optical alignment pointer*

SCALABILITY

Depending on the application requirement, the MiniTrak II™ can be optioned with a single pyrheliometer, or fully equipped to measure all constituent global solar irradiance components in the horizontal and/or POA modes. Such system scalability offers maximum application potential, particularly for the solar renewable resource assessment community, where technology and mounting orientation with respect to the Sun are often quite varied. A 'PV Rack' option is also available for the MiniTrak II™, permitting the mounting and real-world efficiency testing of user supplied PV panels (to one square meter) in the standard two-axis tracking mode (normal incidence), single axis mode (azimuth tracking only), or fixed angle stationary mode.

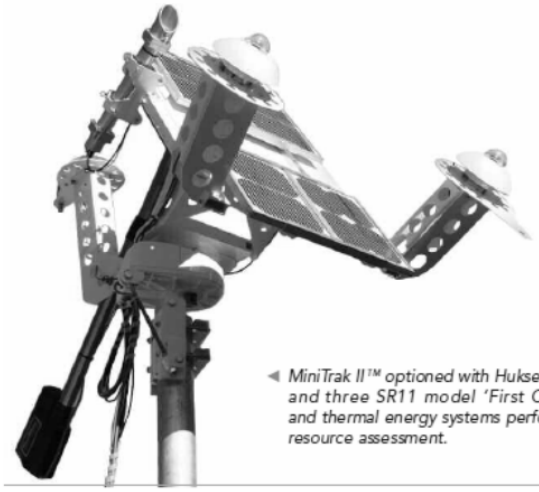

◀ *MiniTrak II™ optioned with Hukseflux DR01 model 'First Class' pyrheliometer and three SR11 model 'First Class' pyranometers, ideal for solar PV and thermal energy systems performance testing and high accuracy solar resource assessment.*

PERFORMANCE

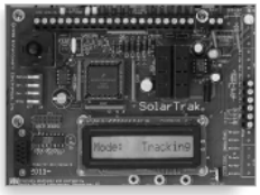

When properly installed and maintained, the MiniTrak II™ will accurately point and consistently maintain any DNI mounted radiometer to within ± 0.25° of the Sun; this represents an order of magnitude 2 times greater than is actually required for a 'First Class' pyrheliometer. The key to the MiniTrak's positioning accuracy is the PST embedded SolarTrak® control electronics, which calculates the bearing of the Sun to within ± 0.01°. The MiniTrak II™ system clock maintains an outstanding accuracy to within ± 15 seconds per year, thus greatly reducing the need for regular routine maintenance.

RELIABILITY

Unlike grid connected tracking systems, which are subject to AC line transient effects, brownouts and blackouts, the MiniTrak II™ draws power from its own integrated solar PV rechargeable DC battery system. So reliable is the MiniTrak II™, PST offers an unprecedented 5-year warranty 'standard' on parts and labor. The MiniTrak's internal system power can also be used to power a data logger, or active sensors requiring DC power.

P.O. Box 850
Manorville, NY 11949

T: 631-251-6963
F: 631-657-0364

E: info@HuksefluxUSA.com
W: www.HuksefluxUSA.com

HuksefluxUSA™
Thermal Sensors

Appendix C: Experiment Measurements

Linear Potentiometers Used in Angle Measurements

Linear Motion Potentiometer **Series - MSL38**

Conductive Plastic Element

Used in Zomeworks UTR-020 Azimuth Angle Measurement

Used in Wattsun AZ-225 Elevation Angle Measurement

- ***100 to 2000mm Stroke Lengths***
- ***Floating Wiper (rodless) with Swivel Joint***
- ***100 Million Cycles Life Span***
- ***High Precision***
- ***Adjustable Mounting Cleats***

Rodless (no shaft) design saves in overall length dimension compared to standard reciprocating shaft designs. Unique swivel joint takes up misalignment play. Robust construction. 10 m/s standard displacement speed.

Electrical Specifications	**100**	**150**	**200**	**300**	**400**	**500**	**750**	**900**	**1000**	**1500**	**2000**
Electrical Stroke (mm)	103	153	204	305	406	509	763	915	1017	1521	2021
Resistance Value (Kohms)	5				10					20	
Resistance Tolerance	±20%										
Linearity Tolerance	±0.1%					±0.05%					
Resolution	Essentially infinite (<0.01mm)										
Output Smoothness	<0.1% against input voltage										
Power @ 40º (W)	3										
Temperature Coefficient	400 ppm/K (actual effect on output voltage <1.5ppm/ºC)										
Insulation Resistance	>100 Mohm @ 500 VDC										
Dielectric Strength	1 minute @ 500 VAC										
Maximum Voltage	60 (V)										
Maximum Wiper Current	10mA (momentarily only)										
Rated Wiper Current	<1µA										
Mechanical Specifications	**100**	**150**	**200**	**300**	**400**	**500**	**750**	**900**	**1000**	**1500**	**2000**
Mechanical Stroke (mm)	113	163	214	315	416	519	773	925	1027	1531	2031
Maximum Operating Friction	1.2 (N)										
Repeatability	0.01mm										
Life Expectancy	25 million meters or 100 million cycles, whichever occurs first										
Displacement Speed	10 m/s										
Vibration	20 g / 5Hz to 2,000 Hz (shaft retracted)										
Shock	50 g / 11ms										
Environmental Specifications											
Operating Temperature	-30ºC to +100ºC										
Storage Temperature	-50ºC to +120ºC										
IP Protection Grade	IP40										
Materials											
Housing	Aluminum										
Shaft	Stainless steel										
Dimension Table (mm)	**100**	**150**	**200**	**300**	**400**	**500**	**750**	**900**	**1000**	**1500**	**2000**
A	113	163	214	315	416	519	773	925	1027	1531	2031
B	253	303	354	455	556	659	913	1065	1167	1671	2171
Weight (kg)	0.5	0.58	0.65	0.8	0.95	1.1	1.5	1.7	1.85	2.6	3.8
Dimensions (mm)											

Direct Normal Irradiation (DNI) Measurement

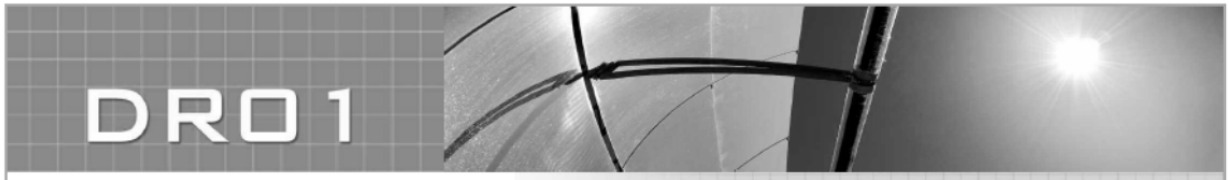

DR01

FIRST CLASS PYRHELIOMETER

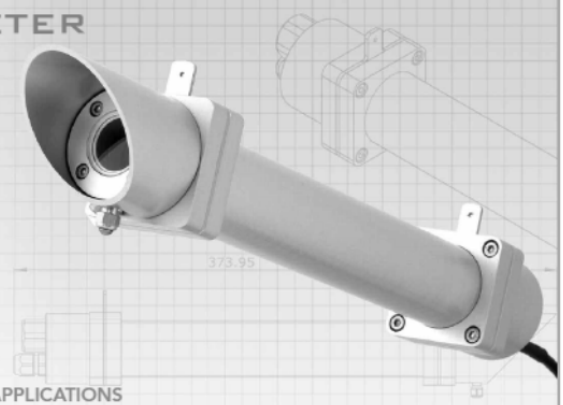

The DR01 is a research grade normal incidence direct solar irradiance sensor (also known as a pyrheliometer). Suitable for tracker mounted operation, the DR01 is intended for short-wave direct solar irradiance measurement of the Sun. The DR01 is a 'First Class' compliant pyrheliometer, as per the latest ISO and WMO standards.

The DR01 foreoptic assembly features a precision ground and polished quartz window/lens, for true spectral solar transmission ranging from 0.2 - 4.0 µm. As per the latest ISO-9060 and WMO standards, the full opening view angle of the DR01 is collimated precisely to 5.0° degrees, making the sensor ideally suited for normal incidence direct solar irradiance measurement. Capable of measuring up to two suns, 2000 W/m², the DR01 pyrheliometer can be deployed anywhere on Earth. The instrument employs a passive thermopile-based sensing technology that generates a low level DC millivolt output signal proportional to the normal incident direct solar flux received at the detector surface. The DR01 also features a thermally isolated low power window/lens heater in the foreoptic; when cycled on/off prior to sunrise the heater effectively eliminates the formation of dew on the pyrheliometer window/lens, thus resulting in improved post sunrise early morning measurement accuracy. Determining direct solar disk irradiance with the DR01 requires connection to a data acquisition device with a measurement resolution of ten micro-volts or better, and an autonomous two-axis solar tracker platform. Typical DR01 measurement applications include scientific meteorological/climate observations, material testing research, solar collector/PV panel efficiency and solar renewable resource assessment validation. The signal cable of the DR01 can be easily replaced by the user onsite, thus minimizing down-time and expense otherwise associated with instrument re-cabling and/or cable connector replacement by the manufacturer. Each DR01 is calibrated upon manufacture and delivered standard with a WRR (World Radiometric Reference) traceable certificate of calibration.

APPLICATIONS

- **Climatology / Meteorology**
- **Material Testing Research**
- **Solar Collector & PV Panel Efficiency Validation**
- **Solar Renewable Resource Assessment**

Note: Above applications are inclusive of, but not limited to the entire DR01 application range.

DR01 SPECIFICATIONS

ISO classification:	First Class
Spectral range:	200 to 4000 nm
Sensitivity (nominal):	10 µV/W/m²
Response time:	4 sec. (1/e signal) 18 sec. (95%)
Range:	0 to 2000 W/m²
Full opening view angle:	5.0° degrees
Slope angle:	1.0° degree
Non-linearity (to 1000 W/m²):	± 1%
Temperature range:	-40 to +80° C
Temperature dependence:	< ± 0.1 %/°C
Non stability (drift):	< ± 1% per year
Calibration traceability:	WRR
Cable length:	5 meter standard *(longer lengths optional)*

OPTIONS

Additional cable length by the meter, AC100 / AC420 amplifiers

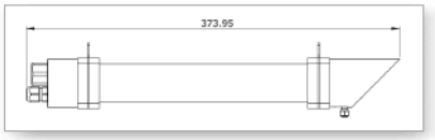

◀ *Figure 1: DR01 Pyrheliometer mechanical dimensions*

P.O. Box 850
Manorville, NY 11949

T: 631-251-6963
F: 631-657-0364

E: info@HuksefluxUSA.com
W: www.HuksefluxUSA.com

HuksefluxUSA™
Thermal Sensors

Global Horizontal Irradiance (GHI) Measurement

LI-200SA Pyranometer Sensor

LI-COR, Inc. Toll Free: 1-800-447-3576 (U.S. & Canada) • Phone: 402-467-3576 • FAX: 402-467-2819 • E-mail: envsales@env.licor.com • Internet: http://www.licor.com

Total Solar Radiation

The LI-200SA Pyranometer is designed for field measurement of global solar radiation in agricultural, meteorological, and solar energy studies. In clear unobstructed daylight conditions, the LI-COR pyranometer compares favorably with first class thermopile type pyranometers (1, 2), but is priced at a fraction of the cost.

Patterned after the work of Kerr, Thurtell and Tanner (3), the LI-200SA features a silicon photovoltaic detector mounted in a fully cosine-corrected miniature head. Current output, which is directly proportional to solar radiation, is calibrated against an Eppley Precision Spectral Pyranometer (PSP) under natural daylight conditions in units of watts per square meter (w m^{-2}). Under most conditions of natural daylight, the error is <5%.

The spectral response of the LI-200SA does not include the entire solar spectrum (Figure 1), so it must be used in the same lighting conditions as those under which it was calibrated. Therefore, the LI-200SA should only be used to measure unobstructed daylight. It should NOT be used under vegetation, artificial lights, in a greenhouse, or for reflected solar radiation.

LI-200SA Specifications

Calibration: Calibrated against an Eppley Precision Spectral Pyranometer (PSP) under natural daylight conditions. Typical error under these conditions is ± 5%.

Sensitivity: Typically 90 µA per 1000 W m^{-2}.

Linearity: Maximum deviation of 1% up to 3000 W m^{-2}.

Stability: < ± 2% change over a 1 year period.

Response Time: 10 µs.

Temperature Dependence: 0.15% per °C maximum.

Cosine Correction: Cosine corrected up to 80° angle of incidence.

Azimuth: < ± 1% error over 360° at 45° elevation.

Tilt: No error induced from orientation.

Operating Temperature: -40 to 65°C.

Relative Humidity: 0 to 100%.

Detector: High stability silicon photovoltaic detector (blue enhanced).

Sensor Housing: Weatherproof anodized aluminum case with acrylic diffuser and stainless steel hardware.

Size: 2.38 Dia. × 2.54 cm H (0.94" × 1.0").

Weight: 28 g (1 oz).

Cable Length: 3.0 m (10 ft).

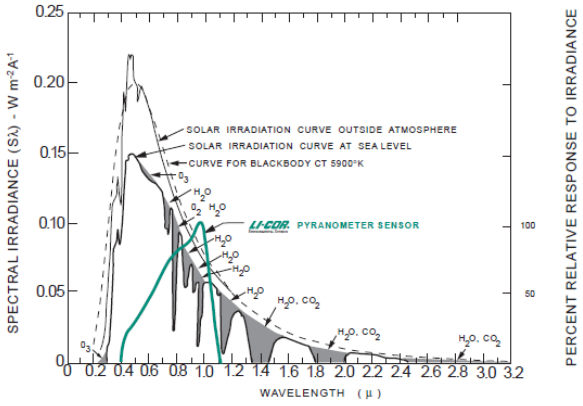

Figure 1. The LI-200SA Pyranometer spectral response is illustrated along with the energy distribution in the solar spectrum (3).

Ordering Information

The LI-200SA Pyranometer Sensor cable terminates with a BNC connector that connects directly to the LI-250 Light Meter or LI-1400 DataLogger. The 2220 Millivolt Adapter should be ordered if the LI-200SA will be used with a strip chart recorder or datalogger that measures millivolts. The 2220 uses a 147 ohm precision resistor to convert the LI-200SA output from microamps to millivolts. The sensor can also be ordered with bare leads (without the connector) designated LI-200SZ. Both are available with 50 foot cables, LI-200SA-50 or LI-200SZ-50. The 2003S Mounting and Leveling Fixture is recommended for each sensor unless other provisions for mounting are made. Other accessories are described on the Accessory Sheet.

LI-200SA Pyranometer
LI-200SZ Pyranometer
LI-200SA-50 Pyranometer
LI-200SZ-50 Pyranometer
2220 Millivolt Adapter
2003S Mounting and Leveling Fixture
2222SB-50 Extension Cable
2222SB-100 Extension Cable

Temperature and Relative Humidity Probe

Model HMP50

The HMP50, manufactured by Vaisala, measures air temperature with a 1000 ohm platinum resistance thermometer (PRT), and RH with the INTERCAP® capacitive chip. The chip is field-replaceable, as needed, and eliminates the downtime typically required for the recalibration process.

Sensor Mounts

When exposed to sunlight, the HMP50 must be housed in a 41303-5A 6-plate radiation shield. To attach the radiation shield directly to a tripod mast, tower mast, or tower leg, place the u-bolt in the side holes. To attach the 41303-5A to a CM202, CM204, or CM206 crossarm, place the 41303-5A's u-bolt in the bottom holes.

Ordering Information

HMP50-L	Temperature and RH Probe with user-specified lead length. Enter the lead length, in feet, after the -L. For example, HMP50-L9 orders a 9 ft lead length.
41303-5A	6-Plate Gill Radiation Shield
9598	Replacement chip for the HMP50.

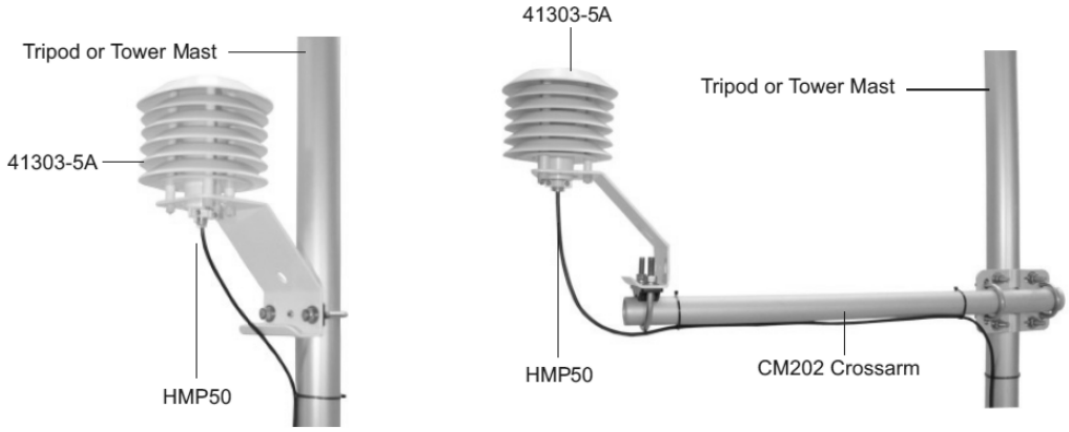

Recommended Lead Lengths

2 m Height		Atop a tripod or tower via a 2 ft crossarm such as the CM202							
Mast/Leg	CM202	CM6	CM10	CM110	CM115	CM120	UT10	UT20	UT30
9'	11'	11'	14'	14'	19'	24'	14'	24'	37'

Note: Add two feet to the cable length if you are mounting the enclosure on the leg base of a light-weight tripod.

Specifications

Relative Humidity

Operating Range: 0 to 98% RH

Accuracy: 0-90% range: ±3.0%
90-98% range: ±5.0%

Temperature Dependence of Relative Humidity Measurement:

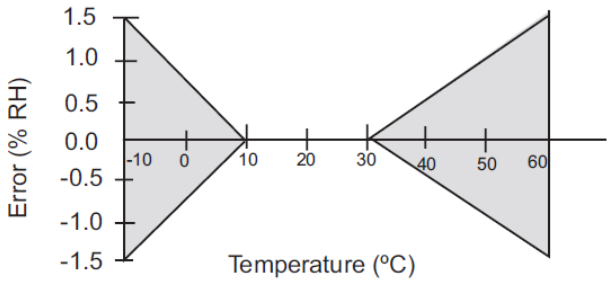

Typical Long-Term Stability: Better than ±1% RH per year

Temperature

Measurement Range: -25° to +60°C

Temperature Accuracy:

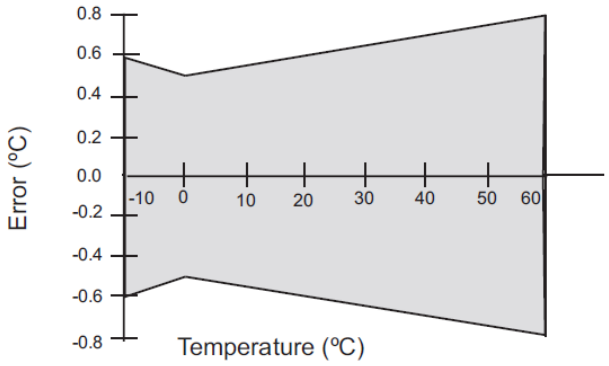

General

Supply Voltage: 7 to 28 Vdc (typically powered by datalogger's 12 V supply)

Current Consumption: 2 mA typical

Diameter: 0.47" (1.2 cm)

Length: 2.8" (7.1 cm)

Housing Material: chrome-coated aluminum and chrome-coated ABS plastic

Vita

Muhammad Sabry was born in Bozeman, Montana in November 1986 when his father was seeking his Doctor of Philosophy degree at Montana State University. Muhammad went to Egypt with his Egyptian father and family after his father had finished his degree. Muhammad completed his education in Egypt, graduating from B-Karnak School for Languages in Cairo, Egypt in 2004. Muhammad completed his Bachelor of Science degree in mechanical power engineering in 2009 at Ain Shams University, Cairo, Egypt. His senior project was designing conventional and unconventional fire protection systems for educational and residence buildings. He sought employment as sales and later worked as a mechanical engineer in the Engineering Construction Office, one of the best electromechanical construction companies in Egypt. After that, Muhammad worked as a technical benchmarking specialist in the Egyptian Electric Utility and Consumer Protection Regulatory Agency. In summer 2011, Muhammad was admitted by the Department of Technology and Environmental Design, Appalachian State University, Boone, North Carolina as a graduate student. In spring 2012, Muhammad returned back to his country of birth and began attending his classes seeking a Master of Science degree with a concentration in renewable energy engineering. Muhammad got involved in several activities and student clubs on campus and in the department and completed his M.S. in August 2013.